Journal of Hazardous Materials

Degradation of difenoconazole in water and soil: kinetics, degradation pathways, transformation products identification and ecotoxicity assessment

--Manuscript Draft--

Manuscript Number:	HAZMAT-D-21-02141R2
Article Type:	Research Paper
Keywords:	Difenoconazole; UHPLC-QTOF/MS; transformation product; degradation pathway; Toxicity
Corresponding Author:	Xingang Liu Institute of Plant Protection, Chinese Academy of Agriculture Sciences Beijing, CHINA
First Author:	Yanli Man
Order of Authors:	Yanli Man
	Marianne Stenrød
	Chi Wu
	Marit Almvik
	Roger Holten
	Jihong Liu Clarke
	Shankui Yuan
	Xiaohu Wu
	Jun Xu
	Fengshou Dong
	Yongquan Zheng
	Xingang Liu
Abstract:	Difenoconazole is a widely used triazole fungicide that has been frequently detected in the environment, but comprehensive study about its environmental fate and toxicity of potential transformation products (TPs) is still lacking. Here, laboratory experiments were conducted to investigate the degradation kinetics, pathways, and toxicity of transformation products of difenoconazole. 12, 4 and 4 TPs generated by photolysis, hydrolysis and soil degradation were identified via UHPLC-QTOF/MS and the UNIFI software. Four intermediates TP295, TP295A, TP354A and TP387A reported for the first time were confirmed by purchase or synthesis of their standards, and they were further quantified using UHPLC-MS/MS in all tested samples. The main transformation reactions observed for difenoconazole were oxidation, dechlorination and hydroxylation in the environment. ECOSAR prediction and laboratory tests showed that the acute toxicities of four novel TPs on Brachydanio rerio , Daphnia magna and Selenastrum capricornutum are substantially lower than that of difenoconazole, while all the TPs except for TP277C were predicted chronically very toxic to fish, which may pose a potential threat to aquatic ecosystems. The results are important for elucidating the environmental fate of difenoconazole and assessing the environmental risks, and further provide guidance for scientific and reasonable use.

Graphical Abstract

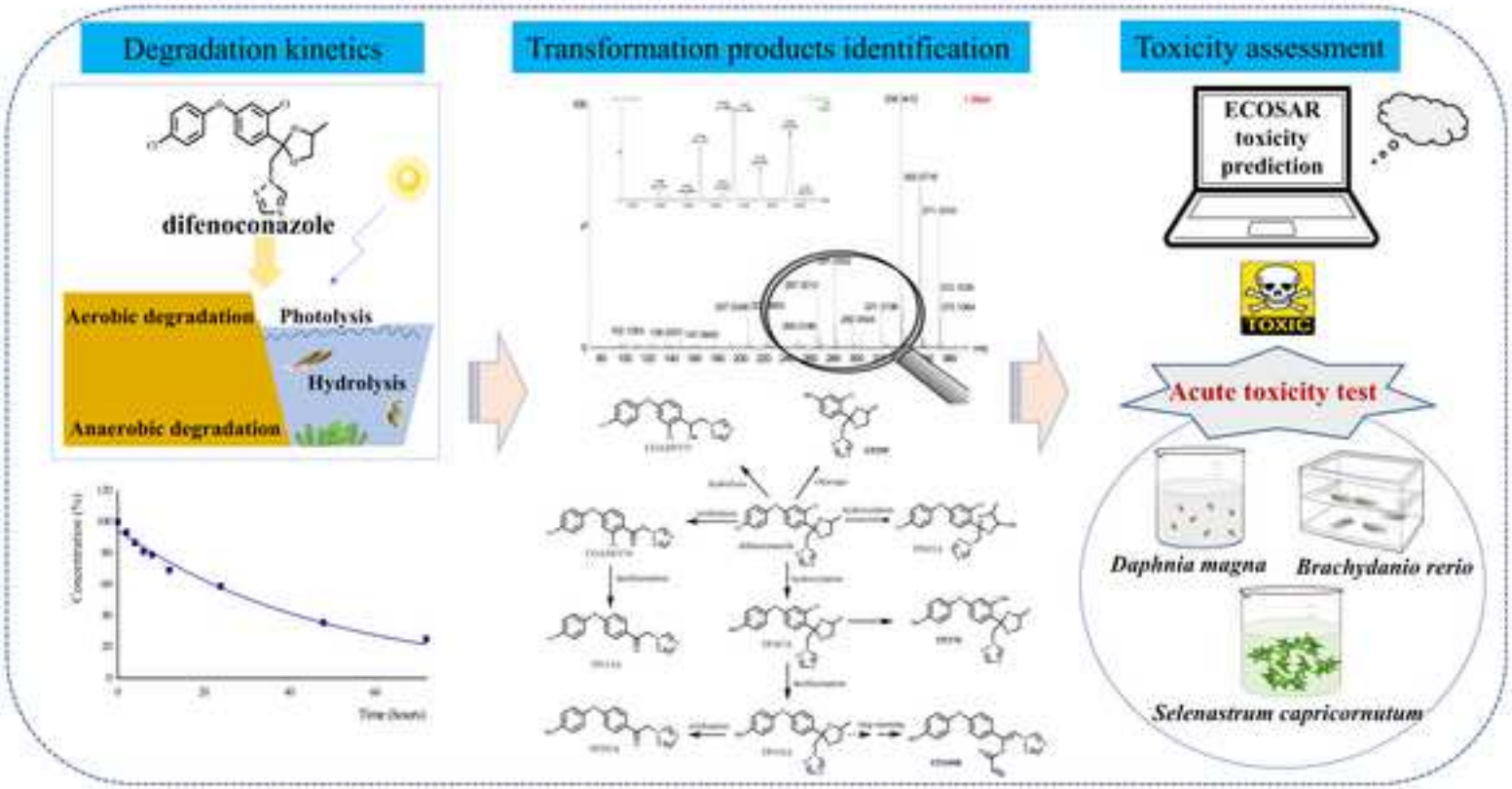

Highlights

Difenoconazole degrade faster under neutral or alkaline solutions and is stable in soils

Four new transformation products were identified and confirmed by standards

Transformation products are produced by oxidation, dechlorination and hydroxylation

The degradation of difenoconazole reduces its toxicity to aquatic organisms

Eleven phototransformation products could still be toxic to aquatic life

This is the accepted version of Man, Y., Stenrød, M., Wu, C., Almvik, M., Holten, R., Clarke, J. L., ... Liu, X. (2021). Degradation of difenoconazole in water and soil: Kinetics, degradation pathways, transformation products identification and ecotoxicity assessment. Journal of Hazardous Materials, 418, 126303. The version of record can be accessed at http://dx.doi.org/10.1016/j.jhazmat.2021.126303

Degradation of difenoconazole in water and soil: kinetics, degradation pathways, transformation products identification and ecotoxicity assessment

Yanli Man [1], Marianne Stenrød [2], Chi Wu [1], Marit Almvik [2], Roger Holten [2], Jihong Liu Clarke[2], Shankui Yuan[3], Xiaohu Wu [1], Jun Xu [1], Fengshou Dong [1], , Yongquan Zheng [1,] *, Xingang Liu [1,] *

[1] *State Key Laboratory for Biology of Plant Disease and Insect Pests, Institute of Plant Protection, Chinese Academy of Agricultural Sciences, Beijing 100193, China.*

[2] *Norwegian Institute of Bioeconomy Research (NIBIO), Division Biotechnology and Plant Health, Høgskoleveien 7, 1433 Aas, Norway*

[3] *Environment Division, Institute for the Control of Agrochemicals, Ministry of Agriculture and Rural Affairs, Beijing 100125, China*

* Corresponding author: Prof, Xingang Liu and Prof. Yongquan Zheng, No. 2 West Yuanmingyuan Road, Institute of Plant Protection, Chinese Academy of Agricultural Sciences, Haidian District, Beijing, PR China.

Tel.: +86 10 62815938; fax: +86 10 62815938.

E-mail address: liuxingang@caas.cn (X. Liu), yqzheng@ippcaas.cn (Y. Zheng)

Abstract: Difenoconazole is a widely used triazole fungicide that has been frequently detected in the environment, but comprehensive study about its environmental fate and toxicity of potential transformation products (TPs) is still lacking. Here, laboratory experiments were conducted to investigate the degradation kinetics, pathways, and toxicity of transformation products of difenoconazole. 12, 4 and 4 TPs generated by photolysis, hydrolysis and soil degradation were identified via UHPLC-QTOF/MS and the UNIFI software. Four intermediates TP295, TP295A, TP354A and TP387A reported for the first time were confirmed by purchase or synthesis of their standards, and they were further quantified using UHPLC-MS/MS in all tested samples. The main transformation reactions observed for difenoconazole were oxidation, dechlorination and hydroxylation in the environment. ECOSAR prediction and laboratory tests showed that the acute toxicities of four novel TPs on *Brachydanio rerio*, *Daphnia magna* and *Selenastrum capricornutum* are substantially lower than that of difenoconazole, while all the TPs except for TP277C were predicted chronically very toxic to fish, which may pose a potential threat to aquatic ecosystems. The results are important for elucidating the environmental fate of difenoconazole and assessing the environmental risks, and further provide guidance for scientific and reasonable use.

Key words: difenoconazole; UHPLC-QTOF/MS; transformation product; degradation pathway; toxicity

1. Introduction

Difenoconazole is a systemic triazole fungicide with high efficiency and high persistence (Dong et al., 2013). It is widely used for disease control in agricultural crops, fruits and vegetables and has been fully recognized worldwide for its high activity and broad-spectrum mode of action enabling control of a wide range of fungi (Pan et al., 2017). Due to the widespread use and stable chemical properties of difenoconazole, it is often detected in environmental samples such as soil, surface water and groundwater at concentrations that range from $\mu g \cdot L^{-1}$ to $mg \cdot L^{-1}$ (Kahle et al., 2008; Satapornvanit et al., 2004; Zhang et al., 2011). For example, Pan (Pan et al., 2019) analysed various types of soil samples in typical farmland in northern China and found that over 1% of the soil sample concentrations exceeded 0.1 $mg \cdot kg^{-1}$. The detected concentration of difenoconazole was as high as 300 $\mu g \cdot L^{-1}$ in drainage water that surrounded paddy fields in Malaysia one week after application (Khalidah Ab et al., 2010). Difenoconazole with *Daphnia magna* chronic NOEC = 0.0056 mg a.s./L is recognized as very toxic to aquatic organisms. It has been reported that difenoconazole has adverse effects on the embryonic development of zebrafish (*Brachydanio rerio*), and it can also inhibit the weight gain of male and female zebrafish. In addition, long-term exposure to difenoconazole can significantly inhibit the growth of adult zebrafish (Mu et al., 2013; Mu et al., 2015). CGA205375, known as 1-(2-(2-chloro-4-(4-chloro-phenoxy)-phenyl)-2-1H-(1,2,4)triazol-yl)-ethanol, is a relevant metabolite formed in soil and is well studied with fish acute EC_{50} = 0.74 mg a.s./L (EFSA, 2011). CGA71019, known as 1,2,4-triazole, is a TP of major fraction and formed in soil, it is also toxic to aquatic organisms with fish chronic NOEC = 3.2 mg a.s./L (EFSA, 2011). According to the data from PPDB (Lewis et al., 2016), difenoconazole is stable against hydrolysis at pH 5 to pH 9, also aqueous photolysis at pH7 and persistent in soil. But the half-life of difenoconazole in field soils is within 30 days (He et al., 2016; Zhao et al., 2018). Until now, studies regarding potential transformation products and pathways of difenoconazole in different water and soils are still limited. If some unknown TPs are persistent in the environment, they may be of great significance to conduct risk assessment. Further studies are needed to assess the fate of difenoconazole, investigate its degradation mechanism and identify transformation products (TPs) in the environment. By providing improved data for environmental risk assessment this will aid in developing a safe and sustainable use practice for this widely used fungicide.

One pesticide may have different degradation rates, pathways and mechanisms

under different environmental conditions (Alletto et al., 2006; Tiwari and Guha, 2014), and the TPs are not necessarily identical among environmental matrices (Ma et al., 2021). It is well known that TPs of organic pesticides are formed by abiotic and biotic processes and are increasingly identified in the environment (Fenner et al., 2013). Pesticides and their TPs are frequently detected in soil, groundwater and surface water, and they represent an important source of chemical pollution (Fenner et al., 2013; Huntscha et al., 2008). Several studies investigated pesticide TPs and their toxicities and showed that TPs might pose similar or even higher toxic effects on different species (Bustos et al., 2019; Escher and Fenner, 2011; Gutowski et al., 2015). Therefore, these substances may pose a greater risk to the environment than their parent compounds. Hensen et al. (Hensen et al., 2020a) demonstrated that TPs increase the number of substances that need to be considered within risk assessment. However, toxicity assessment of pesticide TPs remains a neglected aspect in pesticide registration and application approval (Ji et al., 2020). If there is no information of pesticide degradation, it would be a challenge to explore the fate and ecological effects of pesticides. Under the circumstances, Exposure- or effect-driven approaches (Escher and Fenner, 2011) and hybrid approaches of a combination of in vitro and in silico methods (Gutowski et al., 2015; Hensen et al., 2020b) were developed to evaluate the toxicity of pesticide TPs, and QSAR is also increasingly used for the assessment of environmental properties of pesticide TPs (Jose Villaverde et al., 2017; Villaverde et al., 2018). To predict the fate of pesticides in the natural environment and to access the environmental risks they might pose, it is necessary for us to improve the understanding of the chemical reactions and TP structures of pesticides under various environmental conditions (Sevilla-Moran et al., 2010).

In recent years, high-performance liquid chromatography-time of flight mass spectrometry (UHPLC-QTOF/MS) has played an increasingly important role in environmental analysis (Lim et al., 2016; Storck et al., 2016). The MS^E method was configured to enable data acquisition with two collision energy conditions (high energy and low energy) in parallel to obtain both precursor ions and fragment ions (Bade et al., 2015; Bauer et al., 2018). With the advantages of high sensitivity, high resolution and accurate mass measurements, it can not only screen target compounds but also analyse the structures of unknown degradation or transformation products in combination with elemental analysis (Bade et al., 2015). Powerful data processing and analysis software are required to facilitate sample analysis with these instruments. These systems can

investigate the presence of many contaminants by adding databases of empirical or theoretical compounds without relying on preselected analytes or available reference standards (Hernandez et al., 2014). In this study, an automated software tool Waters UNIFI^{TM}1.8.0 was used to search for TP compounds. Xenon arc lamps are commonly used as a light source to simulate natural light in photolysis studies due to their continuous spectrum and close match to sunlight (Hensen et al., 2019). PH is one of the important factors that affect the degradation of pesticides in water. Considering that the pH value range of natural water is typically 4~9(USEPA, 2008), hydrolysis and photolysis experiments were conducted in buffer solutions with various pH values. Quantitative structure-activity relationship (QSAR) models are potential tools that can predict the activities and properties of chemicals (Furuhama et al., 2010). In this study, ECOSAR was chosen because it is the most extensively validated and used QSAR that can give an automatic prediction of toxicity (Porcelli et al., 2008), and it has previously been successfully applied to evaluate the toxicity of degradation intermediates (Wang et al., 2021; Yang et al., 2021). ECOSAR v1.11 software of the US Environmental Protection Agency (EPA) was used to conduct a preliminary assessment of the aquatic toxicity of the newly identified TPs of difenoconazole.

The objective of this study was to comprehensively analyse the degradation pathways and TPs of difenoconazole produced by biotic degradation in soil and by abiotic transformation in water, i.e. photolysis and hydrolysis. The TPs were predicted and tentatively identified via UHPLC-QTOF/MS and the software UNIFI, and further confirmed by available standards. Furthermore, ECOSAR was used to predict the toxicity of TPs to three aquatic organisms *(Brachydanio rerio*, *Daphnia magna* and *Selenastrum capricornutum*. In addition, acute toxicity tests on aquatic organisms were conducted in laboratory for the TPs with available standards to accurately evaluate their potential risks. These results will provide guidance for further investigation of the degradation pathways and the environmental risk assessment of difenoconazole, and enable a more sustainable and safer use.

2. Materials and methods

2.1 Reagents and chemicals

Standard difenoconazole (purity 99.1%) and CGA205375 (purity 99.1%) were purchased from Beijing Qinchengyixin Technology Co. Ltd., and the TP CGA205374 (purity 99.4%) was obtained from Wuxi Apptec (Shanghai, China). The newly identified TPs of difenoconazole, namely, TP387A (purity 95.45%), TP354A (purity

99.9%), TP295 (purity 97.5%), and TP295A (purity 99.9%), were synthesized by Wuxi Apptec. All stock solutions were prepared in acetonitrile and stored at 4°C in the dark. Acetonitrile (HPLC grade) was purchased from Sigma Aldrich (Steinheim, Germany), and ultrapure grade water was prepared using a Milli-Q reagent water system (Bedford, MA, USA). All analytical reagents including potassium hydrogen phthalate ($C_8H_5KO_4$), sodium hydroxide (NaOH), sodium chloride (NaCl), potassium phosphate monobasic (KH_2PO_4), boric acid (H_3BO_3), hydrochloric acid (HCl), anhydrous magnesium sulfate ($MgSO_4$) and potassium chloride (KCl) for the preparation of buffer solutions were obtained from Beijing Chemical Company (Beijing, China), and all buffer solutions were prepared with Milli-Q water.

2.2 Hydrolysis experimental procedure

Clark-Lubs buffer solutions (pH 4, pH 7 and pH 9 solutions) (Supplementary materials) reported previously (Song et al., 2019) were used in the hydrolysis experiment. The buffer solutions and ultrapure water (pH=7.82) were used as solvents to prepare 5 $mg \cdot L^{-1}$ difenoconazole solutions. All containers were sterilized. The difenoconazole solutions were placed in brown glass bottles and sealed after gentle stirring. These bottles were placed into an incubator with the temperature maintained at 25 ℃ in the dark. 2 mL of each sample was taken from its bottle at the preselected sampling times (day 0, 1, 3, 5, 7, 14, 21, 30, 42, 60, 90, 120, 150 and 180) for the subsequent extraction and analysis. Max 180 d for hydrolysis is to identify more potential transformation products and observe their variation tendency. All the treatments were conducted in triplicate.

2.3 Photodegradation experimental setup and procedure

In our study, photodegradation experiments were conducted in an XT5409-XPC150 xenon arc lamp test chamber (Hangzhou, China) that was equipped with a cooling fan to maintain a stable temperature inside the reactor. The photoreactor used a xenon arc lamp (1000 W with emission at 290 nm~800 nm and the light intensity of 4000 lux) as the irradiation source and could accommodate twenty-four quartz tubes in a merry-go-round apparatus.

Difenoconazole solutions with an initial concentration of 5 $mg \cdot L^{-1}$ were prepared in pH buffers (pH 4, 7 and 9) and ultrapure water (pH=7.82). The photodegradation tests under xenon lamps were conducted using 30 mL quartz tubes that were filled with 25 mL of the solutions. Simultaneously, control experiments in the dark were included to rule out other types of dark reactions. The temperature was maintained at 25 ± 0.5 ℃.

Buffer solutions (pH 4, pH 7 and pH 9 solutions) were freshly prepared prior to use. 2 mL of each sample was collected from the quartz tube at the designated sampling times (0, 2, 4, 6, 8, 12, 24, 48, 72, 120 and 168 hours) for subsequent extraction and analysis. All the treatments were conducted in triplicate.

2.4 Difenoconazole degradation in various soils

The soil degradation experiment was based on the Test Guidelines on Environmental Safety Assessment for Chemical Pesticides – part 1: Transformation in soils. (GB/T 31270.1-2014). Various types of soils - black soil, red soil and fluvo-aquic soil from typical farmlands without the use of difenoconazole - were collected from Harbin in Heilongjiang Province, Changsha in Hunan Province and Langfang in Hebei Province. After air drying and sieving, soil samples were stored in the dark. Information on the soil physicochemical properties is presented in Table 1. Prior to use, ultrapure water was added to achieve 40% of the soil saturated water capacity. The soil was preincubated in the dark to enrich the microbial community for 14 days at 25°C.

For the degradation experiment under aerobic conditions, a suitable amount of a 1000 mg/L difenoconazole stock solution that was prepared with acetone was added to a labelled brown jar that contained 20.0 g of soil, to make an initial concentration of 5 $mg \cdot kg^{-1}$. After vortex mixing and solvent evaporation, the soil moisture content was adjusted with ultrapure water to 60% of the saturated soil moisture content. The bottles were stoppered with cotton and stored in the dark in a PRX-1500D incubator (GREEN, Shanghai, China) under constant temperature (25°C) and humidity. The water content was monitored regularly during soil incubation to maintain the initial state of soil moisture. A corresponding degradation experiment was performed under anaerobic conditions, where water was added to the bottles to a level of 1 cm above the soil surface. The water level was monitored and adjusted when needed to keep the water level constant. Other experimental conditions were identical to those used under aerobic conditions. Triplicate sample bottles of each treatment were taken after pre-determined incubation times (day 0, 1, 3, 5, 7, 14, 30, 42, 60, 90, 120 and 150) and soil samples were freeze dried and stored until extraction. All the soil extraction were further analysed for more comprehensive and accurate identification of TPs.

2.5 Sample preparation procedure

For the hydrolysis and photodegradation samples, 2 mL acetonitrile were added to centrifuge tubes containing 2 mL of water/buffer sample and the tubes were vortexed for 5 min. Then, 1.0 g NaCl was added to each mixture, and the tubes were vortexed

again for 1 min and centrifuged for 5 min at 2810 ×g. After solution stratification, the upper layer (acetonitrile) was filtered with a 0.22-μm nylon syringe filter (Agela, Tianjin, China) and was finally transferred to a brown autosampler vial for UHPLC-QTOF/MS injection.

For soil samples, 10 g of a freeze-dried soil sample was weighed into a 50 mL Teflon centrifuge tube, 5 mL ultrapure water was added. The tube was allowed to stand for 10 min. Then, 10 mL acetonitrile was added as the extractant, and the tube was capped immediately and shaken vigorously for 10 min. Four grams of anhydrous $MgSO_4$ and 1 g of NaCl were then added to the tube, and the mixture was shaken for 1 min and centrifuged for 5 min at 2810 ×g. Subsequently, 1.5 mL of the supernatant was transferred into a 2 mL centrifuge tube that was filled with 50 mg PSA and 150 mg anhydrous $MgSO_4$. The extracts were vortexed again for 1 min and centrifuged for 5 min at 2292 ×g. Finally, the supernatants of the prepared samples were filtered with a 0.22-μm nylon syringe filter and were transferred to a brown autosampler vial for UHPLC-QTOF/MS injection.

2.6 Instrumentation and conditions

2.6.1 UHPLC-MS/MS conditions

The concentrations of difenoconazole and its identified TPs in water and soil samples were analysed by a Waters Acquity UHPLC system coupled with a triple quadrupole mass spectrometer ((TQD, Waters Corp., Milford, MA, USA). A Waters Acquity UHPLC BEH C18 column (2.1 × 100 mm 1.7-μm particle size; Milford, MA, USA) was used for separation. The mobile phase was 0.1% formic acid in water (A) and acetonitrile (B), and the flow rate was set at 0.3 $mL \cdot min^{-1}$. The gradient program was set as follows: 0-1.0 min: hold 10% B; 1.0-3.0 min: linear gradient to 90% B; 3.0-3.1 min: linear gradient to 10% B; 3.1-5.0 min: hold 10% B. The injection volume was 3 μL, and the column temperature was maintained at 40℃. The target compounds (Table 2) were analyzed under positive electrospray ionization (ESI+) in the multi reaction monitoring mode (MRM). Quantification of target compounds were determined using multipoint matrix-matched (water and soil) calibration curves.

2.6.2 UHPLC-QTOF/MS conditions

The TPs were screened using a UHPLC system (Acquity UHPLC, Waters Corp., Milford, MA, USA) coupled with a quadrupole time-of-flight mass spectrometer (QTOF, Waters, Milford, MA, USA) in this study. A Waters Acquity UHPLC BEH C18 column (2.1 × 100 mm 1.7-μm particle size; Milford, MA, USA) was used for

separation. The gradient of solvent A (0.1% (v/v) formic acid in water) and solvent B (chromatography-grade acetonitrile) was as follows: 0-1.0 min: hold 10% B, 1.0-8.0 min: linear gradient to 90% B, 8.0-11.0 min: hold 90% B, 11.0-12.0 min: linear gradient to 10% B, 12.0-14.0 min: hold 10% B. The flow rate was set to 0.3 mL/min, the injection volume was 5 μL, and the column temperature was maintained at 40°C.

An electrospray ionization (ESI) source was operated in positive ionization and resolution mode. To realize the maximum transmission of precursor ions, tuning parameters were optimized. The following parameters were used: capillary voltage, 3.0 kV; cone voltage, 20 V; desolvation temperature, 350°C; source temperature, 150°C; desolvation gas flow rate, 600 L/h; cone gas flow rate, 0 L/h; low collision energy (precursor ions), 4 eV; and high collision energy (product ions), 10–45 eV. A 0.5 mM sodium formate solution in 90:10 2-propanol/water was used for mass axis calibration, and leucine enkephalin (reference m/z is 556.2771 in positive mode) was used as the external lock mass for real-time mass correction. Data were acquired from m/z 50 to 1200 Da at a scan speed of 1.0 s in MS^E continuum mode.

2.7 Acute toxicity experiment

The toxicities of difenoconazole and its four TPs (TP295, TP295A, TP354A, TP387A) to three aquatic organisms (*B. rerio*, *D. magna Straus* and *S. capricornutum*) were determined according to the OECD Guidelines for the Testing of Chemicals, Test No. 203 (OECD, 2019), Test No. 202 (OECD, 2011) and Test No. 201 (OECD, 2004). To improve the solubilization, dimethyl formamide was used to solubilize these substances to obtain concentrated stock solutions. The stock solution of each substance was diluted to a series of concentrations with dechlorinated tap water or BG11 medium. Three replicates were performed at each concentration. Additional controls were included containing the solvent with the highest concentration that was used in the experimental group.

ECOSAR was used to predict the acute and chronic toxicities of difenoconazole TPs to aquatic organisms. By inputting the SMILES notation, the new substance is assigned to a chemical class defined by the ECOSAR, and the predicted results are generated.

2.8 Data analysis

This method adopted non-targeted screening to collect mass spectrometry data with high quality accuracy, which enabled us to improve the identification efficiency of metabolites. The rawfiles with precursor ions and product ions data that were obtained

from the high-resolution mass spectrometry were imported into UNIFI^{TM} v1.8.0 (Waters Corp., Milford, MA, USA), which contained a scientific library with predicted molecular structure, formula and precise molecular weight for screening and identification of TPs. The binary comparison function of UNIFI was used to compare the control samples and the treated samples, and highlight the significantly different and unique substances in the treated samples. The TrendPlot function was used to create trendlines of the transformation products throughout the sampling time periods, and the transformation products were further identified by the help of the corresponding chromatograms, mass spectra and structural information records in UNIFI. In addition, the common fragments search function efficiently extracted the components with common structural characteristics.

Several degradation kinetic models, single first order (SFO), double first-order in parallel (DFOP) and first-order multiple compartments model (FOMC), were used to describe the degradation kinetics and to determine the half-life (DT_{50}) of difenoconazole. The three model equations are given in supplementary materials. The Computer Aided Kinetic Evaluation (CAKE) R-based software was used to obtain the half-lives and degradation rates.

According to Globally Harmonized System of Classification and Labeling of Chemicals (GHS) (United Nations, 2011), predicted toxicity values in the ranges of <1 $mg \cdot L^{-1}$, 1-10 $mg \cdot L^{-1}$, 10-100 $mg \cdot L^{-1}$ and >100 $mg \cdot L^{-1}$ are classified into “Category 1, very toxic”, “Category 2, toxic”, “Category 3, harmful” and “not classified for acute/long-term hazard” to aquatic life, respectively. SPSS 19.0 software Probit (probability unit method) (Wu et al., 2020) was used for the statistical calculation of LC_{50} or EC_{50}.

3. Results and discussion

3.1 Analysis method validation

Linearity was evaluated by constructing calibration curves with concentrations that ranged from 0.01-5 $mg \cdot L^{-1}$ for difenoconazole and 0.001-1 mg/L for its identified TPs (CGA205374, CGA205375, TP295, TP295A, TP354A and TP387A). All the curves demonstrated highly satisfactory linearity ($R^2 \geq 0.9995$ for all the tested analytes) on UHPLC-MS/MS. Recovery experiments with four spiking levels, namely, 0.001, 0.01, 0.1 and 5 $mg \cdot kg^{-1}$, for various buffer solutions and soils were used to validate the method. Each level was tested in five replicates. The mean recoveries of difenoconazole and all six TPs at various levels from an aquatic solution ranged from 95.1% to 118.6%,

with relative standard deviations (RSDs) that ranged from 1.4% to 16.2%. The mean recoveries of difenoconazole, CGA205375 and TP295 from three soils were in the range of 75.6%~109.6%, and the RSDs were in the range of 1.5%~10.1%. The results demonstrated that the analysis methods can be used to detect the concentrations of difenoconazole and its TPs simultaneously in environmental matrices with satisfactory recovery, precision and sensitivity.

3.2 Degradation kinetics of difenoconazole in water and soil

The photolysis of difenoconazole in aquatic solutions was well fitted by single first order (SFO) kinetic model (R^2 values 0.9856 to 0.9957). The DT_{50} values of 33.8 h, 14.6 h, 16.6 h and 13.7 h were obtained at initial pH 4, pH 7, pH 9 and ultrapure water, respectively. The reaction rate constant (k) and the corresponding correlation coefficient (R^2) are given in table S1. The photodegradation rate of difenoconazole was faster than that reported in the literature, this may be caused by different experimental conditions such as various buffer salts and radiation sources etc. The degradation of difenoconazole under neutral and alkaline conditions was significantly faster than that under acidic conditions, this may be because OH^- free radicals can promote the photolysis of difenoconazole to some extent under irradiation. This also can explain the results of the hydrolysis, the hydrolysis of difenoconazole probably occurs when the nucleophilic group (H_2O or OH^-) in water attacks the electrophilic group (chlorine-carbon atom), resulting in a bimolecular nucleophilic substitution reaction (Li et al., 2020). However, a slower degradation followed an initial rapid degradation in the hydrolysis experiments. The SFO kinetics did not sufficiently describe the apparently bi-phasic hydrolysis process and the DFOP and FOMC models (Table S2) provided better fits overall and resulted in DT_{50} values that agreed better with observed values. We assume that this behavior could actually be related to the sorption of difenoconazole to the brown bottles during the hydrolysis experiment. DFOP model was more reasonable to describe the hydrolysis kinetics. And the DT_{50} values of difenoconazole hydrolysis in pH 4, pH 7, pH 9 solutions and ultrapure water were 31.6 d, 5.79 d, 28 d and 7.7 d in the DFOP model.

Types of soil differ in their abilities to degrade pesticides (Kah et al., 2007). The results (Fig S2) demonstrated that difenoconazole can remain stable in all three soils with different physicochemical properties under both aerobic and anaerobic conditions over 150 days of incubation. The results are not the same as data showing that the half-lives of difenoconazole were in the range of 10.3–21.2 d in non-sterilized soils (Zhang

et al., 2021). Differences in soil properties, microbial communities and preculture conditions may cause discrepancy. Under anaerobic conditions, almost no degradation occurred in the three soils. Under aerobic conditions, the degradation of difenoconazole was much faster than that in anaerobic conditions. After 150 days of aerobic incubation, the degradation rate of difenoconazole under aerobic conditions in black soil was the highest, which was followed by that in fluvo-aquic soil, and the degradation rate was the slowest in red soil. Obviously, a fast initial decrease in difenoconazole concentration was followed by a slower decline in black and fluvo-aquic soils under aerobic conditions, which exhibited two-phase degradation behaviour. This may be related to the high organic contents of these two soils, which are favourable for microbial activity, but they can also easily adsorb difenoconazole and make it less available for microbial degradation (Fushiwaki and Urano, 2001). The biphasic kinetics (DFOP and FOMC) were used to describe difenoconazole degradation in fluvo-aquic soil and black soil (Fig. S3). Soil is a complex system, very similar fit of DFOP and FOMC models suggests that the degradation is likely to occur in two compartments as assumed by the two models. There is great uncertainty in DT_{50} values (>1000 days) in the models, because they were outside of the duration of the experiment.

3.3 Identification of TPs

To identify precisely the structures of potential TPs, the extracts of water and soil were evaluated via UHPLC-QTOF/MS to obtain a full scan of the information on the degraded molecule and its ion fragmentations, and they were further analysed by simulating the fragmentation patterns using the UNIFI software. All reported metabolites, transformation products and unknown probable TPs (including tentatively identified compounds) were included in the database of the library of the UNIFI platform. The software simulated the fragmentation patterns of compounds in the database and compared them against experimentally derived fragmentation patterns. During the analysis, new tentative compounds were continuously added into the database on the basis of the previous analysis to identify additional potential compounds. The following criteria were used to filter the potential TP candidates: (1) peaks detected in the unknown samples (the treatment) but not in the controls or at significantly lower levels in the controls, (2) the concentration showed an increasing trend or the concentration initially increased and subsequently decreased with the extension of the incubation time, (3) satisfactory peak shape, (4) the mass error of precursor ion m/z < ± 3 mDa, (5) characteristic isotopic peaks, (6) ≥ 2 common fragments matched, and

(7) the retention time of the precursor ion did not deviate more than 0.1 min in all samples.

Based on the fitted molecular formulas, MS/MS fragmentation patterns and reasonable fragment loss regulations, the tentative structure of each TP was obtained. According to the above screening criteria, a total of 14 TPs were tentatively identified. All the tentatively identified as well as identified TPs of difenoconazole are listed in Table 3. Among these identified compounds, two of them were previously reported by Joint FAO/WHO Meeting on Pesticide Residues (JMPR, 2007): 1-(2-chloro-4-(4-chloro-phenoxy)-phenyl)-2-(1,2,4-triazol)-1-ylethanone (CGA205374) and 1-[2-chloro-4-(4-chloro-phenoxy)-phenyl]-2-(1,2,4-triazol)-1-yl-ethanol (CGA205375). CGA205375 was detected in all three soil samples under both aerobic and anaerobic conditions, and CGA205374 was detected in the photolysis of water samples. Four of the TPs, namely, TP295, TP295A, TP354A and TP387A, were synthesized by WuXi AppTec to assess their toxicity. These TPs were further verified by comparing the retention times, chromatograms and mass spectra of the standards with those of the tentative compounds in the samples.

A molecular ion with m/z $[M + H]^+$ 296.0803, namely, TP295, was detected in in various buffer solutions and all soil degradation samples. The isotopic abundance ratio between the M and M + 2 peaks is 3:1, which shows that the structure contains only a single chlorine atom. We infer that the other chlorine atom was removed from the parent structure. The resulting data, which were processed using the UNIFI software, suggested that the chemical formula was $C_{13}H_{14}ClN_3O_3$ and the total degree of unsaturation was reduced by 4 compared with the parent compound. This was likely caused by the cleavage of the ether linkage between the two benzene rings. Based on the analysis, the structure of TP295 was proposed and imported into the library. There are 7 common fragments in the stimulated and practical secondary mass spectra.

Two TPs of m/z 388.10566 (TP387A) and m/z 354.1449 (TP354A) were detected at 5.48 min and 5.10 min, respectively. The fragmentation patterns facilitated the identification of the molecular structures of degradation intermediates. The major fragments of TP387A exhibited m/z 109.02658, 205.03871, 233.03406, 247.01171 and 319.07158, which corresponded to the elemental compositions of $[C_6H_5O_2]^+$, $[C_{12}H_{10}ClO]^+$, $[C_{11}H_8ClN_3O]^+$, $[C_{11}H_6ClN_3O_2]^+$ and $[C_{17}H_{16}ClO_4]^+$, respectively. The major fragments of TP354A exhibited m/z 121.06578, 171.08029, 197.05984, 199.07519, 213.05519 and 285.11320, which corresponded to the elemental

compositions of $[C_8H_9O]^+$, $[C_{12}H_{11}O]^+$, $[C_{11}H_7N_3O]^+$, $[C_{11}H_9N_3O]^+$, $[C_{11}H_7N_3O_2]^+$, and $[C_{16}H_{15}O_4]^+$, respectively. Through a comparative analysis of the fragment ions and structural screening, it is speculated that the two products result from the dechlorination and substitution of hydroxyl groups. They are presumed to be 4-(4-(2-((1H-1,2,4-triazol-1-yl) methyl)-4-methyl-1,3-dioxolan-2-yl) phenoxy) phenol and 4-(4-(2-((1H-1,2,4-triazol-1-yl)methyl)-4-methyl-1,3-dioxolan-2-yl)-3-chlorophenoxy) phenol. A compound with m/z 296.10344 and a retention time of 4.49 min, namely, TP295A, was observed in photolysis samples of pH 7 and ultrapure water solutions, and the molecular formula was $C_{16}H_{13}N_3O_3$. The dioxolane structure, which is linked by a chiral carbon, may be oxidized to a carbonyl group by ring-opening; moreover, two chlorine atoms fall off the benzene ring, and one is replaced by a hydroxyl group. We posited that substance TP295A is 1-(4-(4-hydroxyphenoxy) phenyl)-2-(1H-1,2,4-triazol-1-yl) ethan-1-one. Finally, custom-synthesized standards were used to confirm the four proposed structures (TP295, TP295A, TP354A and TP387A). A comparison of the retention time and mass spectrum information between standard and experimental molecules indicated that they are in satisfactory accordance with each other (Fig 1). Additional ^{1}H-NMR spectra of these compounds for structural identification are provided in Fig S5-S9.

Additionally, several TPs that had not been previously reported in the literature in photolysis and soil degradation samples were identified. For technical reasons, the remaining 8 TPs could not be synthesized; hence, they are restricted to the level of inference.

3.4 Quantification of TPs

An MRM method with UHPLC-MS/MS for qualitative and quantitative analyses of difenoconazole and its six identified TPs was developed to confirm their structures once again. In the photodegradation of difenoconazole with an initial concentration of 5 $mg \cdot L^{-1}$ in ultrapure water, as shown in Fig 2, the concentrations of most TPs initially increased and subsequently decreased; hence, these intermediates were unstable under light. With increasing irradiation time, these TPs inevitably degrade to various degrees. For example, the concentration of TP387A reached 0.076 $mg \cdot L^{-1}$ (2% of the applied amount of parent) at 4 h, but the compound disappeared after 7 days. However, in contrast to the above products, TP295A showed an increasing trend throughout the whole experiment, and on the 7th day, the concentration was close to 0.02 $mg \cdot L^{-1}$ (1% of the applied amount of parent). The same trend was observed in a pH 7 buffer. The

concentration of TP387A reached 0.5 mg·L^{-1} (12.1% of the applied amount of parent) at 48 h under acidic pH 4 conditions. It is speculated that acidic conditions are more favourable for the formation of the product TP387A. The concentrations of TP295 and TP387A in alkaline solutions reached their highest values of 0.01 mg·L^{-1} (no more than 1% of the applied amount of parent) and 0.02 mg·L^{-1} (no more than 1% of the applied amount of parent) in the first 6 h and subsequently decreased until the compounds disappeared. However, TP295A and CGA205374 were not detected in alkaline solutions. In the hydrolysis experiment, CGA205374, TP295, TP354A and TP387A were also observed, but they could not be accurately quantified because they appeared in mid to late stage of hydrolysis with much lower concentrations which were below the LOQs. It is inferred that difenoconazole and its TPs may take a long time to degrade due to the limited conditions in natural water with various pH values. Difenoconazole has strong adsorption capacity and weak mobility in soil (Wang et al., 2020) and this also might be the case for some of the TPs, they may sorb to sediments/particles and precipitate from the water phase into the sediments in water bodies. Another possibility is that some of TPs may stick around in the water phase because they are usually more polar and water soluble than the parent compound (Boxall et al., 2004).

Although difenoconazole was stable in all three soils in the soil degradation experiment, several potential TPs were still observed. The quantitative results demonstrated that the two TPs (CGA205375 and TP295) accumulated with increasing incubation time in both aerobic and anaerobic environments (Fig 3). However, the formation rates of several TPs under aerobic conditions exceed those under anaerobic conditions. Under anaerobic conditions, the concentrations of CGA205375 in red soil and fluvo-aquic soil were lower than 0.01 mg·kg^{-1} throughout the incubation period. These results indicate that aerobic microorganisms in soil play an important role in the degradation of difenoconazole (Thom et al., 1997). In addition, two products, namely, TP421A and TP387G, that were generated from hydroxylation and dechlorination were also detected in the soil.

3.5 Proposed degradation pathways of difenoconazole in water and soil

The proposed degradation pathways that result from soil degradation, photolysis and hydrolysis in water are illustrated in Fig 4. The results show that difenoconazole may have similar degradation pathways in the three types of soil. This is in line with other published findings, which show that many pesticides have similar degradation pathways in soils with different physical and chemical properties and that the same TPs

are formed in the process of degradation (Kah et al., 2007; Wang et al., 2018). The same is true of photolysis and hydrolysis in this experiment. In our study, the main degradation pathways of difenoconazole in soil included hydrolysis, hydroxylation and cleavage of the ether link between the two benzene rings. These reactions caused the formation of CGA205375, TP421A and TP295, respectively. In addition to the common degradation pathways in soil, many other complex degradation pathways in aqueous solutions under light irradiation were identified. Difenoconazole was phototransformed into CGA205374 via oxidation and to TP313A via dechlorination. Simultaneously, one of the chlorine atoms on the benzene ring was replaced by a hydroxyl group, thereby leading to the formation of TP387A, and the other chlorine atom was removed from the benzene ring to produce TP370. Meanwhile, TP354A was formed due to the hydroxyl substitution reaction of TP387A, and subsequently, a series of oxidations, ring scissions and elimination reactions resulted in TP295A and TP349B. In another degradation pathway, the H atom in the dioxolane structure was replaced by a hydroxyl group to produce TP421A, and dechlorination generated TP387G. The elimination of H_2O led to the formation of a double bond and gave rise to TP369C1, and further hydroxylation finally resulted in the formation of TP351A. Moreover, cleavage of the ether bond of TP387G generated TP277C. The structures of the TPs showed that the dioxolane structure and chlorine atom were more reactive in the difenoconazole structure, while the triazole ring and benzene ring were relatively stable.

3.6 Ecotoxicity assessment of TPs by ECOSAR

Since transformation products generally endow different toxicities, the acute and chronic toxicities of difenoconazole and the studied TPs to fish, daphnid and green algae were predicted using ECOSAR. The results are shown in Table 4. In terms of acute toxicity, most of TPs belong to “toxic” category, though they possess lower acute toxicity to the three aquatic organism groups as compared to the parent compound. Difenoconazole is in “very toxic” and “toxic” categories. TP369C1 is classified as “very toxic” to aquatic life and its acute toxicity to Daphnid is even much higher than that of the parent compound. In addition, TP349B is classified as “very toxic” to green algae. As for chronic toxicity, except for TP277C, all the TPs are classified as “very toxic” compounds for fish. Furthermore, the chronic toxicity of TP349B to fish were approximately the same as difenoconazole and it is classified into “very toxic” category for Daphnid and green algae. All the compounds belong to the category of “very toxic” to Daphnid except TP277C, TP295 and TP295A. Such predictions can help us obtain a

basic understanding of the toxicities of the TPs, although there may be some discrepancies between the predicted value and the results obtained from experimental toxicity studies.

According to the theoretical values, the degradation of difenoconazole reduces its toxicity overall, which agreed with previous studies (Day and Maguire, 1990; Heydens et al., 2000; Mermana et al., 2012). Significantly, when the initial concentration of difenoconazole is 5 $mg \cdot L^{-1}$ in photolysis experiment, TP387A is detected at a maximum of 0.5 $mg \cdot L^{-1}$ in pH 4 buffer which is above the chronic toxicity threshold for fish and Daphnid, and this will inevitably pose a risk to aquatic ecosystems. However, the concentration of difenoconazole may not be as high as 5 $mg \cdot L^{-1}$ in the real environment, and there are many uncertain factors affecting the degradation process. Therefore, further risk assessment is needed to determine whether these TPs such as TP387A indicate a risk of eliciting chronic toxicity effects. Many TPs require further attention due to the high chronic toxicity to aquatic life as shown by the predicted values . More evaluation of the toxicity of TPs toward the ecosystem in the real environment is required.

3.7 Ecotoxicity testing of TPs

To investigate the real toxicity of the TPs, acute toxicity tests of difenoconazole and its identified TPs (TP295, TP295A, TP354A and TP387A) with available standards in the laboratory on aquatic organisms were conducted. The acute toxicity of CGA205374 were not measured due to the small amount of standards. In the zebrafish (*B. rerio*) acute toxicity experiment, the semistatic method of replacing the chemical solution once every 24 h was used. The toxicity symptoms and deaths of *B. rerio* at 24 h, 48 h, 72 h and 96 h were recorded. The 96 h LC_{50} and 48 h EC_{50} values of difenoconazole for *B. rerio* and Daphnia (*D. magna*) were all between 1 mg a.i./L and 10 mg a.i./L, the value for *B. rerio* is consistent with the 48 h LC_{50} (1.41 mg a.i./L) and 96 h LC_{50} (1.45 mg a.i./L) reported by Sanches et al. (2017) and Mu et al. (2013). The 48 h EC_{50} value of difenoconazole for *D. magna* is not exactly the same as the result (0.77 mg a.i./L) reported by EFSA, this may be due to differences between various water systems, use of solvents or test media. The 72 h EC_{50} value of difenoconazole for green algae (*S. capricornutum)* was 2.24 mg a.i./L. The 96 h LC_{50} values of TP295, TP295A, TP354A and TP387A to *B. rerio* were all > 10 mg a.i./L (all the tested individuals survived at a concentration of 10 mg a.i./L in various groups). The results of the acute immobilization test on *D. magna* were similar to those on *B. rerio*, with all

four TPs having 48 h EC_{50} >10 mg a.i./L. It is concluded that the acute toxicities of these TPs to *B. rerio* and *D. magna* are significantly lower than parent compound difenoconazole, and the four TPs are all classified as “harmful” or “not classified for acute/long-term hazard” to *B. rerio* and *D. magna*. Therefore, no values for the 96 h LC_{50} of *B. rerio* or the 48 h EC_{50} of *D. magna* were obtained.

The EC_{50} (72 h) values of TP295, TP354A and TP387A for the growth of *S. capricornutum* were all > 3 mg a.i./L (when the concentration was set at 3 mg a.i./L, no inhibitory effect on the growth of *S. capricornutum* was observed in all the treatment groups). However, the growth inhibition rate of *S. capricornutum* were 10.9% when the concentration of TP295A were 3 mg a.i./L, this indicated that the EC_{50} value of TP295A for the growth of *S. capricornutum* was also > 3 mg a.i./L. In reference to Globally Harmonized System of Classification and Labeling of Chemicals (GHS), TP295, TP354A, TP387A and TP295A to *S. capricornutum* are all belong to category of “harmful” or “not classified for acute/long-term hazard”. Specific values for the 72 h EC_{50} of *S. capricornutum* were not calculated due to the much low toxicity. Although single acute toxicity data do not provide a comprehensive picture of the risk to aquatic organisms of these TPs, the experimental results clearly demonstrated that the toxicity of TP295, TP295A, TP354A and TP387A were substantially lower than that of difenoconazole.

The experimental results are not fully in accordance with the predicted toxicity results (Table 5), which has also been reported by others (Reuschenbach et al., 2008). This may be caused by differences between species and experimental conditions. For TP295A, TP354A and TP387A, the experimental and predicted acute toxicity data of the three aquatic organisms fall into the same toxicity class. The toxicity of difenoconazole to fish and algae and toxicity of TP295 to all the three organisms were overestimated by ECOSAR. The predicted toxicity and the experimental toxicity reported by European Food Safety Authority (EFSA, 2011) of CGA205375 showed that in comparison to fish, the predicted acute toxicity data for Daphnid and algae show a clearly good agreement with the measured data. However, the acute toxicity of CGA205375 to fish was underestimated by ECOSAR. In most cases, ECOSAR provide a conservative estimate of the toxicity (Burden et al., 2016). Although there are errors and miss-estimations, the results show that the toxicity classification proposed by ECOSAR is reliable to a certain extent. For the untested chemicals or substances that have not yet been synthesized, ECOSAR can still provide as preliminary ecological

toxicological data support for further environmental risk assessment.

4. Conclusions

This study is the first time transformation products of a widely used triazole fungicide difenoconazole were determined with the help of UHPLC-QTOF/MS, suggests new degradation pathways involving oxidation, hydrolysis, hydroxylation, dechlorination and cleavage of ether bonds for difenoconazole under environmentally relevant conditions, and provides toxicity data both measured and predicted on novel transformation products. The degradation process of difenoconazole reduces its toxicity overall, but some transformation products with decreased aquatic ecological toxicity are still toxic to different aquatic organisms. This research is an important step forward in the prediction of environmental fate and evaluation of environmental risks of difenoconazole, and it provides technical support and theoretical guidance for scientific and rational use of difenoconazole. It is necessary to fully understand the environmental behavior of pesticides and consider the potential impacts of pesticide TPs on the environment. This study provides scientific basis for environmental fate and environmental risk assessment of pesticides. Furthermore, it provides theoretical guidance for the development of high-activity lead compounds, and has theoretical and practical significance to ensure the safety of agro-ecological environment and agricultural products.

Declaration of interests

The authors declare that they have no known competing financial interests or personal relationships that could have appeared to influence the work reported in this paper.

Acknowledgements

The authors thank The National Natural Science Foundation of China (NSFC 31861133021) and the Research Council of Norway (Project 287431) for financial support. In addition, we are grateful to the Norwegian Ministry of Foreign Affairs through the Royal Norwegian Embassy in Beijing for their support to the Sinograin II project (project ID: CHN 2152, 17/0019).

References

Alletto, L., Coquet, Y., Benoit, P. and Bergheaud, V. 2006. Effects of temperature and water content on degradation of isoproturon in three soil profiles. Chemosphere 64(7), 1053-1061.

Anderson, J.P.E. (1987) Handling and storage of soils for pesticide experiments.

Bade, R., Rousis, N.I., Bijlsma, L., Gracia-Lor, E., Castiglioni, S., Sancho, J.V. and Hernandez, F. 2015. Screening of pharmaceuticals and illicit drugs in wastewater and surface waters of Spain and Italy by high resolution mass spectrometry using UHPLC-QTOF MS and LC-LTQ-Orbitrap MS. Analytical and Bioanalytical Chemistry 407(30), 8979-8988.

Bauer, A., Luetjohann, J., Hanschen, F.S., Schreiner, M., Kuballa, J., Jantzen, E. and Rohn, S. 2018. Identification and characterization of pesticide metabolites in Brassica species by liquid chromatography travelling wave ion mobility quadrupole time-of-flight mass spectrometry (UPLC-TWIMS-QTOF-MS). Food Chemistry 244, 292-303.

Boxall, A.B.A., Sinclair, C.J., Fenner, K., Kolpin, D. and Maud, S.J. 2004. When synthetic chemicals degrade in the environment. Environmental Science & Technology 38(19), 368A-375A.

Burden, N., Maynard, S.K., Weltje, L. and Wheeler, J.R. 2016. The utility of QSARs in predicting acute fish toxicity of pesticide metabolites: A retrospective validation approach. Regulatory Toxicology and Pharmacology 80, 241-246.

Bustos, N., Cruz-Alcalde, A., Iriel, A., Fernandez Cirelli, A. and Sans, C. 2019. Sunlight and UVC-254 irradiation induced photodegradation of organophosphorus pesticide dichlorvos in aqueous matrices. Science of the Total Environment 649, 592-600

Day, K.E. and Maguire, R.J. 1990. Acute toxicity of isomers of the pyrethroid insecticide deltamethrin and its major degradation products to Daphnia magna. Environmental Toxicology and Chemistry 9(10), 1297-1300.

Dong, F., Li, J., Chankvetadze, B., Cheng, Y., Xu, J., Liu, X., Li, Y., Chen, X., Bertucci, C., Tedesco, D., Zanasi, R. and Zheng, Y. 2013. Chiral Triazole Fungicide Difenoconazole: Absolute Stereochemistry, Stereoselective Bioactivity, Aquatic Toxicity, and Environmental Behavior in Vegetables and Soil. Environmental Science & Technology 47(7), 3386-3394.

Escher, B.I. and Fenner, K. 2011. Recent Advances in Environmental Risk Assessment of Transformation Products. Environmental Science & Technology 45(9), 3835-3847.

European Food Safety Authority. 2011. Conclusion on the peer review of the pesticide risk assessment of the active substance difenoconazole. EFSA Journal 9(1),

1967-1967.

Fenner, K., Canonica, S., Wackett, L.P. and Elsner, M. 2013. Evaluating Pesticide Degradation in the Environment: Blind Spots and Emerging Opportunities. Science 341(6147), 752-758.

Furuhama, A., Toida, T., Nishikawa, N., Aoki, Y., Yoshioka, Y. and Shiraishi, H. 2010. Development of an ecotoxicity QSAR model for the KAshinhou Tool for Ecotoxicity (KATE) system, March 2009 version. Sar and Qsar in Environmental Research 21(5-6), 403-413.

Fushiwaki, Y. and Urano, K. 2001. Adsorption of pesticides and their biodegraded products on clay minerals and soils. Journal of Health Science 47(4), 429-432.

Gutowski, L., Olsson, O., Leder, C. and Kuemmerer, K. 2015. A comparative assessment of the transformation products of S-metolachlor and its commercial product Mercantor Gold (R) and their fate in the aquatic environment by employing a combination of experimental and in silico methods. Science of the Total Environment 506, 369-379.

He, M., Jia, C.H., Zhao, E.C., Chen, L., Yu, P.Z., Jing, J.J. and Zheng, Y.Q. 2016. Concentrations and dissipation of difenoconazole and fluxapyroxad residues in apples and soil, determined by ultrahigh-performance liquid chromatography electrospray ionization tandem mass spectrometry. Environmental Science and Pollution Research 23(6), 5618-5626.

Hensen, B., Olsson, O. and Kuemmerer, K. 2019. The role of irradiation source setups and indirect phototransformation: Kinetic aspects and the formation of transformation products of weakly sunlight-absorbing pesticides. Science of the Total Environment 695.

Hensen, B., Olsson, O. and Kümmerer, K. 2020b. A strategy for an initial assessment of the ecotoxicological effects of transformation products of pesticides in aquatic systems following a tiered approach. Environment International 137, 105533.

Hernandez, F., Ibanez, M., Bade, R., Bijlsma, L. and Sancho, J.V. 2014. Investigation of pharmaceuticals and illicit drugs in waters by liquid chromatography-high-resolution mass spectrometry. Trac-Trends in Analytical Chemistry 63, 140-157.

Heydens, W.F., Wilson, A.G.E., Kraus, L.J., Hopkins, W.E. and Hotz, K.J. 2000. Ethane sulfonate metabolite of alachlor: Assessment of oncogenic potential based on metabolic and mechanistic considerations. Toxicological Sciences 55(1), 36-43.

Huntscha, S., Singer, H., Canonica, S., Schwarzenbach, R.P. and Fenner, K. 2008. Input dynamics and fate in surface water of the herbicide metolachlor and of its highly mobile transformation product metolachlor ESA. Environmental Science & Technology 42(15), 5507-5513.

Ji, C., Song, Q., Chen, Y., Zhou, Z., Wang, P., Liu, J., Sun, Z. and Zhao, M. 2020. The potential endocrine disruption of pesticide transformation products (TPs): The blind spot of pesticide risk assessment. Environment International 137.

Jose Villaverde, J., Sevilla-Moran, B., Lopez-Goti, C., Luis Alonso-Prados, J. and Sandin-Espana, P. 2017. Computational Methodologies for the Risk Assessment of Pesticides in the European Union. Journal of Agricultural and Food Chemistry 65(10), 2017-2018.

Kah, M., Beulke, S. and Brown, C.D. 2007. Factors influencing degradation of pesticides in soil. Journal of Agricultural and Food Chemistry 55(11), 4487-4492.

Kahle, M., Buerge, I.J., Hauser, A., Mueller, M.D. and Poiger, T. 2008. Azole fungicides: Occurrence and fate in wastewater and surface waters. Environmental Science & Technology 42(19), 7193-7200.

Khalidah Ab, L., Nor Kartini, A.B. and Nurzawani Md, I. 2010. Preliminary study of difenoconazole residues in rice paddy watersheds. Malaysian Journal of Science 29(1), 73-79.

Li, M., Wang, R., Kong, Z., Gao, T., Wang, F. and Fan, B. 2020. Cyflumetofen degradation in different aquatic environments and identification of hydrolytic products. Journal of Environmental Chemical Engineering 8(6).

Lim, L., Yan, F., Bach, S., Pihakari, K. and Klein, D. 2016. Fourier Transform Mass Spectrometry: The Transformation of Modern Environmental Analyses. International Journal of Molecular Sciences 17(1).

Ma, C., Liu, X., Wu, X., Dong, F., Xu, J. and Zheng, Y. 2021. Kinetics, mechanisms and toxicity of the degradation of imidaclothiz in soil and water. Journal of Hazardous Materials 403, 124033.

Mermana, J., Sutthivaiyakit, P., Blaise, C. and Gagne, F. 2012. Photo-catalysis of propanil under simulated solar light: formation of degradation products and toxicity implications. Fresenius Environmental Bulletin 21(12), 3618-3625.

Mu, X., Pang, S., Sun, X., Gao, J., Chen, J., Chen, X., Li, X. and Wang, C. 2013. Evaluation of acute and developmental effects of difenoconazole via multiple

stage zebrafish assays. Environmental Pollution 175, 147-157.

Mu, X., Wang, K., Chai, T., Zhu, L., Yang, Y., Zhang, J., Pang, S., Wang, C. and Li, X. 2015. Sex specific response in cholesterol level in zebrafish (Danio rerio) after long-term exposure of difenoconazole. Environmental Pollution 197, 278-286.

United Nations. 2011 Globally Harmonized System of Classification and Labelling of Chemicals (GHS), 4th ed. United Nations Publications.

OECD (2004) Test No. 202: Daphnia sp. Acute Immobilisation Test.

OECD (2011) Test No. 201: Freshwater Alga and Cyanobacteria, Growth Inhibition Test.

OECD (2019) Test No. 203: Fish, Acute Toxicity Test.

Pan, L., Feng, X., Cao, M., Zhang, S., Huang, Y., Xu, T., Jing, J. and Zhang, H. 2019. Determination and distribution of pesticides and antibiotics in agricultural soils from northern China. Rsc Advances 9(28), 15686-15693.

Pan, L., Lu, L., Wang, J., Zheng, C., Fu, Y., Xiao, S., Jin, Y. and Zhuang, S. 2017. The fungicide difenoconazole alters mRNA expression levels of human CYP3A4 in HepG2 cells. Environmental Chemistry Letters 15(4), 673-678.

Porcelli, C., Boriani, E., Roncaglioni, A., Chana, A. and Benfenati, E. 2008. Regulatory perspectives in the use and validation of QSAR. A case study: DEMETRA model for Daphnia toxicity. Environmental Science & Technology 42(2), 491-496.

Reuschenbach, P., Silvani, M., Dammann, M., Warnecke, D. and Knacker, T. 2008. ECOSAR model performance with a large test set of industrial chemicals. Chemosphere 71(10), 1986-1995.

Sanches, A.L.M., Vieira, B.H., Reghini, M.V., Moreira, R.A., Freitas, E.C., Espíndola, E.L.G. and Daam, M.A. 2017. Single and mixture toxicity of abamectin and difenoconazole to adult zebrafish (Danio rerio). Chemosphere 188, 582-587.

Satapornvanit, K., Baird, D.J., Little, D.C., Milwain, G.K., Van den Brink, P.J., Beltman, W.H.J., Nogueira, A.J.A., Daam, M.A., Domingues, I., Kodithuwakku, S.S., Perera, M.W.P., Yakupitiyage, A., Sureshkumar, S.N. and Taylor, G.J. 2004. Risks of pesticide use in aquatic ecosystems adjacent to mixed vegetable and monocrop fruit growing areas in Thailand. Australasian Journal of Ecotoxicology 10(2), 85-95.

Sevilla-Moran, B., Alonso-Prados, J.L., Garcia-Baudin, J.M. and Sandin-Espana, P. 2010. Indirect Photodegradation of Clethodim in Aqueous Media. Byproduct

Identification by Quadrupole Time-of-Flight Mass Spectrometry. Journal of Agricultural and Food Chemistry 58(5), 3068-3076.

Song, S., Zhang, C., Chen, Z., Wei, J., Tan, H. and Li, X. 2019. Hydrolysis and photolysis of bentazone in aqueous abiotic solutions and identification of its degradation products using quadrupole time-of-flight mass spectrometry. Environmental Science and Pollution Research 26(10), 10127-10135.

Storck, V., Lucini, L., Mamy, L., Ferrari, F., Papadopoulou, E.S., Nikolaki, S., Karas, P.A., Servien, R., Karpouzas, D.G., Trevisan, M., Benoit, P. and Martin-Laurent, F. 2016. Identification and characterization of tebuconazole transformation products in soil by combining suspect screening and molecular typology. Environmental Pollution 208, 537-545.

Thom, E., Ottow, J.C.G. and Benckiser, G. 1997. Degradation of the fungicide difenoconazole in a silt loam soil as affected by pretreatment and organic amendment. Environmental Pollution 96(3), 409-414.

Tiwari, M.K. and Guha, S. 2014. Kinetics of biotransformation of chlorpyrifos in aqueous and soil slurry environments. Water Research 51, 73-85.

USEPA 2008. Fate, Transport and Transformation Test Guidelines. OPPTS 835.2120. Hydrolysis. EPA 712-C-08-012.

Villaverde, J.J., Sevilla-Morán, B., López-Goti, C., Calvo, L., Alonso-Prados, J.L. and Sandín-España, P. 2018. Photolysis of clethodim herbicide and a formulation in aquatic environments: Fate and ecotoxicity assessment of photoproducts by QSAR models. Science of The Total Environment 615, 643-651

Wang, F., Cao, D., Shi, L., He, S., Li, X., Fang, H. and Yu, Y. 2020. Competitive Adsorption and Mobility of Propiconazole and Difenoconazole on Five Different Soils. Bulletin of Environmental Contamination and Toxicology 105(6), 927-933.

Wang, L., Zhao, J., Delgado-Moreno, L., Cheng, J., Wang, Y., Zhang, S., Ye, Q. and Wang, W. 2018. Degradation andmetabolic profiling for benzene kresoxim-methyl using carbon-14 tracing. Science of the Total Environment 637, 1221-1229.

Wang, W., Chen, M., Wang, D., Yan, M. and Liu, Z. 2021. Different activation methods in sulfate radical-based oxidation for organic pollutants degradation: Catalytic mechanism and toxicity assessment of degradation intermediates. Science of the Total Environment 772.

Wu, W., Kong, D., Zhang, W., Bu, Y., Li, J. and Shan, Z. 2020. Acute toxicity of fluazinam to aquatic organisms and its bioaccumulation inBrachydanio rerio. Environmental Science and Pollution Research 27(28), 35000-35007.

Yang, T., Mai, J., Wu, S., Liu, C., Tang, L., Mo, Z., Zhang, M., Guo, L., Liu, M. and Ma, J. 2021. UV/chlorine process for degradation of benzothiazole and benzotriazole in water: Efficiency, mechanism and toxicity evaluation. Science of the Total Environment 760.

Zhang, H., Song, J., Zhang, Z., Zhang, Q., Chen, S., Mei, J., Yu, Y. and Fang, H. 2021. Exposure to fungicide difenoconazole reduces the soil bacterial community diversity and the co-occurrence network complexity. Journal of Hazardous Materials 405, 124208.

Zhang, Z.-y., Wang, D.-l., Zhang, C.-z., Wu, C.-f. and Liu, X.-j. 2011. Difenoconazole Residues in Rice and Paddy System. Zhongguo Shuidao Kexue 25(3), 339-342.

Zhao, F.F., Liu, J.K., Xie, D.F., Lv, D.Z. and Luo, J.H. 2018. A novel and actual mode for study of soil degradation and transportation of difenoconazole in a mango field. Rsc Advances 8(16), 8671-8677.

Figure captions

Fig. 1. The chromatogram and mass spectra of the transformation products of difenoconazole obtained from samples and their standards. (a) TP295 from sample and standard, (b) TP295A from samples and standard, (c) TP354A from samples and standard and (d) TP387A from samples and standard.

Fig. 2. Dynamic of five transformation products generated from photolysis of difenoconazole in (a) pH4 buffer, (b) pH7 buffer, (c) pH9 buffer and (d) ultra-pure water (pH = 7.82). These compounds were quantified by UHPLC-MS/MS.

Fig. 3. Dynamic of two transformation products generated from difenoconazole degradation in soil，(a) TP295 under aerobic condition, (b) TP295 under anaerobic condition, (c) CGA205375 under aerobic condition and (d) CGA205375 under anaerobic condition. These compounds were quantified by UHPLC-MS/MS.

Fig. 4. Proposed pathway for the degradation of difenoconazole in environment.

Tables

Table 1 The physical and chemical properties of the tested soils from China.

Soil type	Location	Latitude / longitude	Soil texture	pH	CEC/cmol·kg^{-1}	OMC/g·kg^{-1}
Red soil	Hunan	28°12’N,113°5’E	clay	4.30	11.99	6.85
Fluvo-aquic soil	Hebei	39°30’N,116°36’E	Silt loam	5.26	15.79	46.09
Black soil	Heilongjiang	51°55’N,124°35’E	Sandy loam	5.82	41.42	50.97

CEC: Cation exchange capacity
OMC: Organic matter content

Table 2 Experimental parameters and UHPLC–MS/MS conditions of difenoconazole and its transformation products in ESI+ mode.

compound	Molecular formula	t_R(min)	CV(V)	Quantification ion transition	CE1(eV)	Diagnostic ion transition	CE2(eV)
difenoconazole	$C_{19}H_{17}Cl_2N_3O_3$	2.59	40	406.1→251.1	38	406.1→337.1	25
CGA205374	$C_{16}H_{11}C_{l2}N_3O_2$	2.38	35	347.7→250.8	35	347.7→69.7	36
CGA205375	$C_{16}H_{13}Cl_2N_3O_2$	2.31	15	350.02→70.23	22	350.02→281.0	18
TP295	$C_{13}H_{14}ClN_3O_3$	1.76	30	295.7→140.8	28	295.7→227.12	22
TP295A	$C_{16}H_{13}N_3O_3$	1.79	296	296.0→198.8	31	296.0→92.8	45
TP354A	$C_{19}H_{19}N_3O_4$	1.94	27	354.1→199.0	30	354.1→284.9	21
TP387A	$C_{19}H_{18}ClN_3O_4$	2.04	30	387.8→233.0	32	387.8→318.8	28

Table 3 Transformation products of difenoconazole in water and soil. The screening was performed with mass filter error of±3 mDa, retention time error of ± 0.1 min, and at least three common fragments.

Compound name	Structure	Formula	Observed m/z (Da)	Retention time (min)	Mass error (mDa)	Common fragments	Adducts	Confirmation	Sample containing TPs
CGA205374 reported	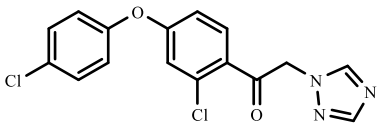	$C_{16}H_{11}Cl_2N_3O_2$	348.0303	6.64	-1.1	70.0395 111.0422 129.0081 141.0079	+H	confirmed	Photolysis，hydrolysis
CGA205375 reported	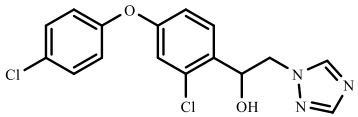	$C_{16}H_{13}Cl_2N_3O_2$	350.0463	6.37	-1.7	70.0395 141.0076 266.9958	+H	confirmed	Soil degradation
TP277C	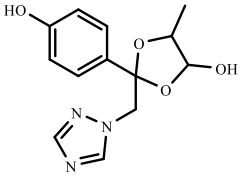	$C_{13}H_{15}N_3O_4$	278.1139	3.30	0.4	123.0436 151.0372 163.0760 209.0807	+H	tentative	Photolysis

TP295	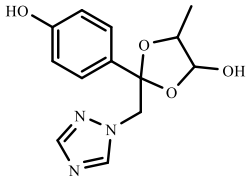	$C_{13}H_{14}ClN_3O_3$	296.0803	4.18	0.6	95.0483 113.0143 154.9876 181.0395 213.0289 227.0452	+H	confirmed	Photolysis，soil degradation, hydrolysis
TP295A	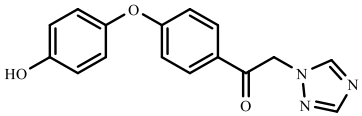	$C_{16}H_{13}N_3O_3$	296.1034	4.49	0.1	171.0811 199.0752 228.0756	+H	confirmed	Photolysis,
TP313A	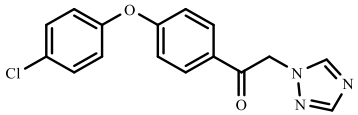	$C_{16}H_{12}ClN_3O_2$	314.0695	5.43	0.4	109.0288 169.0659 185.0584 198.0675 201.0522 233.0366	+H	tentative	Photolysis
TP349B	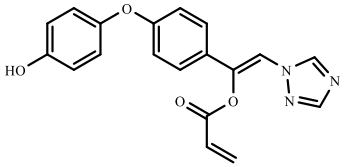	$C_{19}H_{15}N_3O_4$	350.1142	5.43	0.5	94.0415 109.0289 172.0512 201.0523 237.0759 266.0922 282.0875	+H	tentative	Photolysis

TP351A	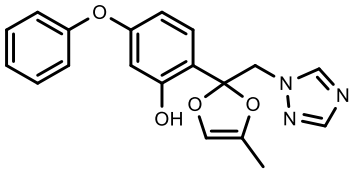	$C_{19}H_{17}N_3O_4$	352.1292	5.39	0.0	94.0415 109.0290 185.0582 201.0523 237.0759 266.0922 294.0877 308.1016	+H	tentative	Photolysis
TP354A	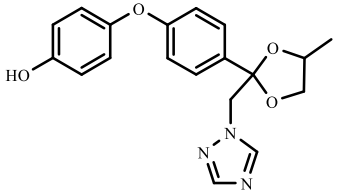	$C_{19}H_{19}N_3O_4$	354.1445	5.11	-0.3	121.0658 171.0803 197.0598 199.0752 213.0552 285.1132	+H	confirmed	Photolysis, hydrolysis
TP369C1	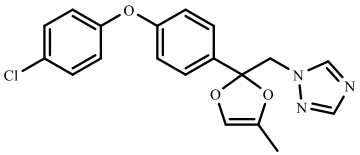	$C_{19}H_{16}ClN_3O_3$	370.0955	6.20	0.2	165.0533 276.0767 283.0520 296.0586 300.0548 311.0456	+H	tentative	Photolysis
TP370	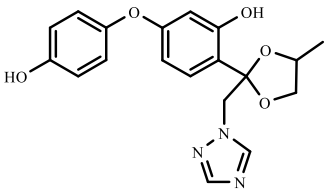	$C_{19}H_{19}N_3O_5$	370.1397	4.32	0.0	168.0769 185.0583 213.0523 282.0880 294.0878	+H	tentative	Photolysis

						312.0965			
TP387A	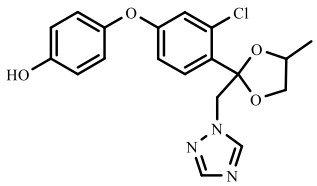	$C_{19}H_{18}ClN_3O_4$	388.1057	5.47	-0.2	109.0266 205.0387 233.0341 319.0716 247.0117	+H	confirmed	Photolysis
TP387G	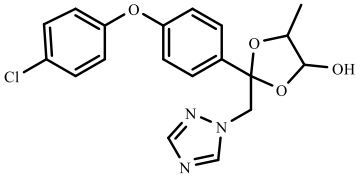	$C_{19}H_{18}ClN_3O_4$	388.1040	7.61	-1.9	89.0587 147.0785 155.0689 244.1103 254.0943 296.0578	+H	tentative	Photolysis， soil degradation
TP421A	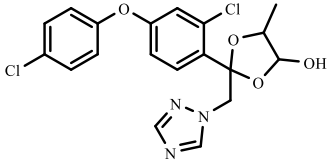	$C_{19}H_{17}Cl_2N_3O_4$	422.0648	6.36	-2.1	155.0682 249.0648 277.0609 343.1079 353.0345	+H	tentative	Soil degradation

Table 4 Predictive acute and chronic toxicities of difenoconazole and its transformation products to aquatic organisms by ECOSAR

compound	Predicted acute toxicity (mg a.i./L)			Predicted chronic toxicity (mg a.i./L)		
	Fish LC_{50} (96 h)	Daphnid EC_{50} (48 h)	Green algae EC_{50} (96 h)	Fish ChV[a]	Daphnid ChV[a]	Green algae ChV[a]
Difenoconazole	0.265	1.069	0.263	0.004	0.028	0.268
CGA205374	2.323	2.914*	1.055	0.017	0.138	1.006
CGA205375	2.799	2.559	1.331	0.022	0.179	1.257
TP277C	479.019	51.055	51.785	1.322	11.668	41.509
TP295	49.575	15.062	10.374	0.221	1.874	8.921
TP295A	35.962	11.852	8.238	0.171	1.444	7.152
TP313A	7.086	4.816	2.134	0.038	0.310	1.966
TP349B	1.552	3.138	0.517	0.004	0.128	0.186
TP351A	1.673	5.297	2.333	0.042	0.338	2.152
TP354A	5.006	2.852	2.109	0.037	0.301	1.953
TP369C1	0.802	0.607	0.599	0.009	0.072	0.528
TP370	5.361	8.075	3.688	0.076	0.623	3.636
TP 387A/TP387G	1.778	1.350	1.031	0.017	0.132	0.988
TP 421A	1.021*	2.124*	0.649*	0.01	0.078	0.637*

[a] Chronic toxicity value. The ChV is geometric mean of no observed effect concentration (NOEC) and the lowest observed effect concentration (LOEC).

* Chemical may be not soluble enough to measure this predicted effect.

Table 5 Comparison of ECOSAR data and measured aquatic toxicity for difenoconazole and its new identified TPs to *B. rerio, D. magna and S. capricornutum*

Compound	*B. rerio* LC_{50} (96 h) (mg a.i./L)		*D. magna* EC_{50} (48 h) (mg a.i./L)		*S. capricornutum* EC_{50} (72 h) (mg a.i./L)	
	Experimental value	Predicted value	Experimental value	Predicted value	Experimental value	Predicted value
Difenoconazole	$1 < LC_{50} < 10$	0.265	$1 < EC_{50} < 10$	1.069	2.24	0.263
TP 295	> 10	2.323	> 10	2.914*	> 3	1.055
TP 295A	> 10	479.019	> 10	51.055	> 3	51.785
TP 354A	> 10	49.575	> 10	15.062	> 3	10.374
TP 387A	> 10	35.962	> 10	11.852	> 3	8.238
CGA205375	0.74 (Rainbow trout)	2.799	1.4	2.559	1.2	1.331

* Chemical may be not soluble enough to measure this predicted effect.

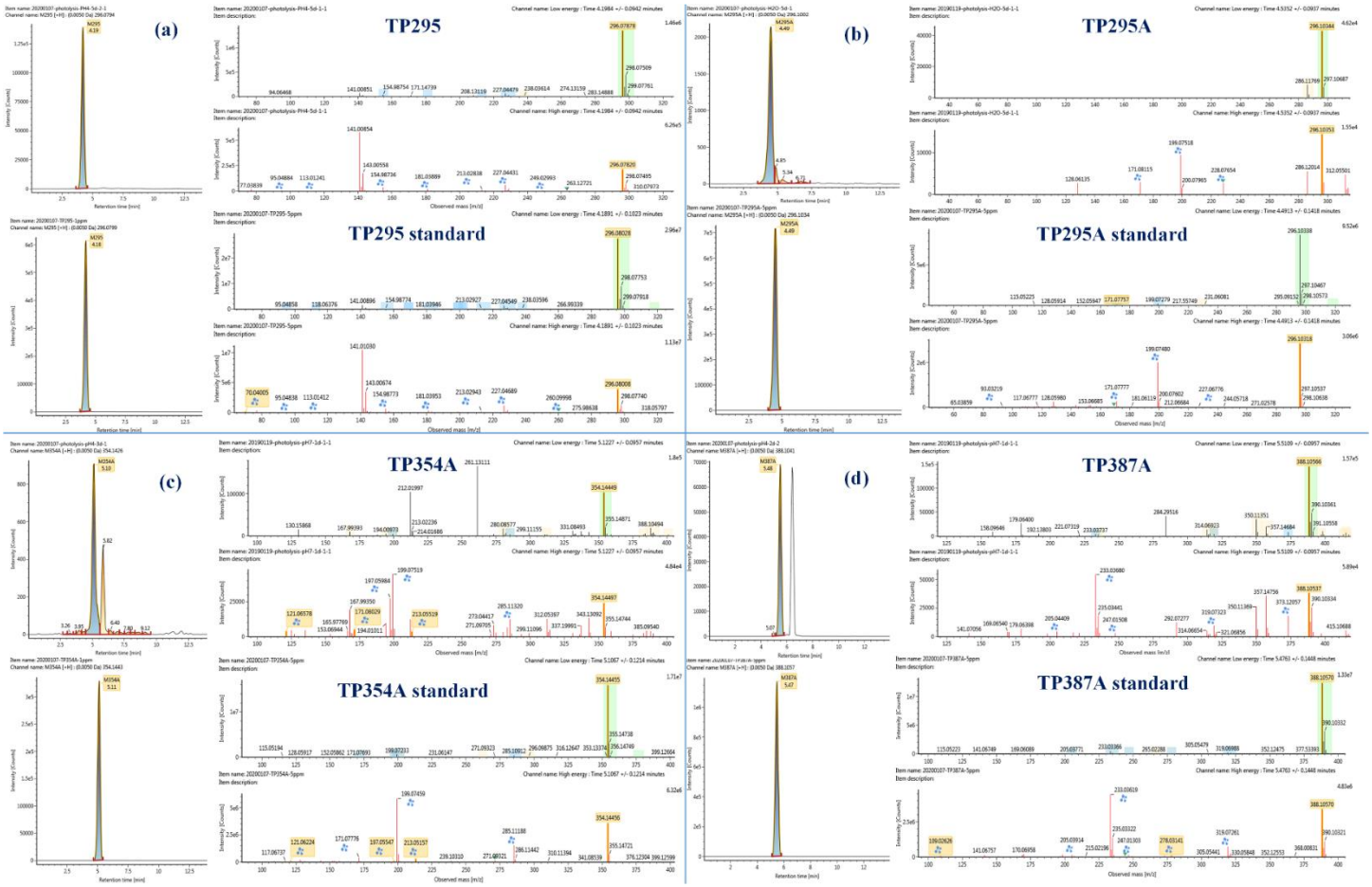

Fig. 1. The chromatogram and mass spectra of the degradation products of difenoconazole obtained from samples and their standards. (a) TP295 from sample and standard, (b) TP295A from samples and standard, (c) TP354A from samples and standard and (d) TP387A from samples and standard.

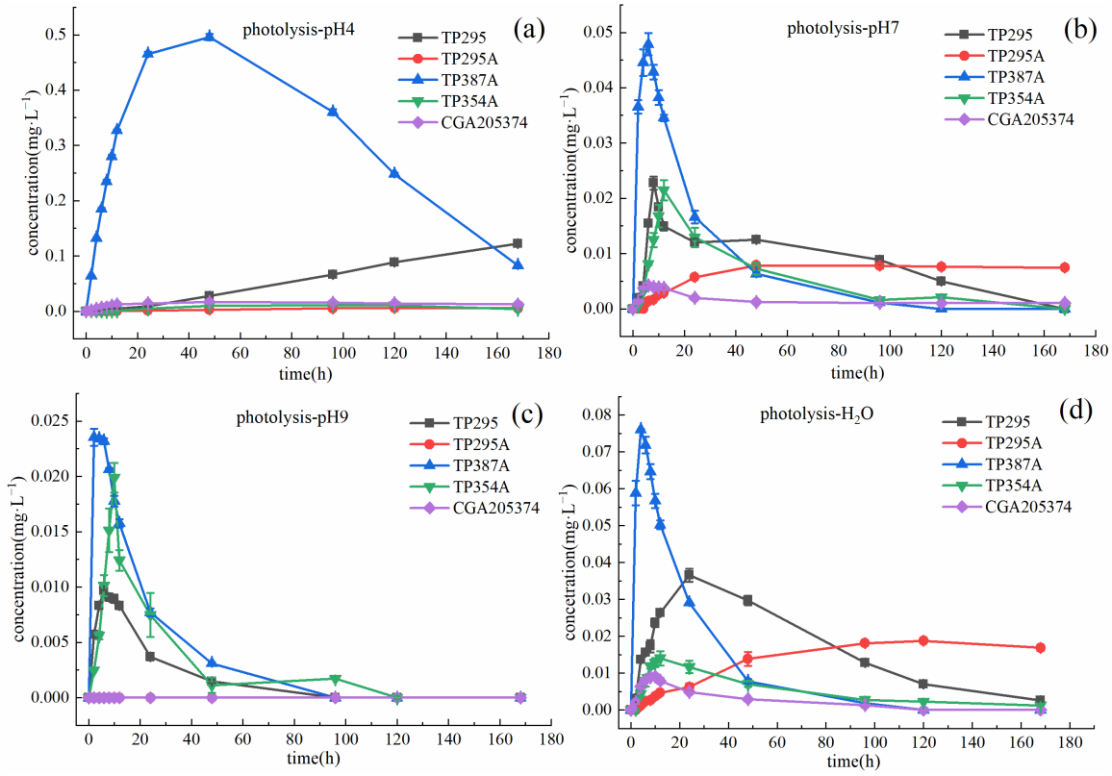

Fig. 2. Dynamic of five degradation products generated from photolysis of difenoconazole in (a) pH4 buffer, (b) pH7 buffer, (c) pH9 buffer and (d) ultra-pure water (pH = 7.82). These compounds were quantified by UHPLC-MS/MS.

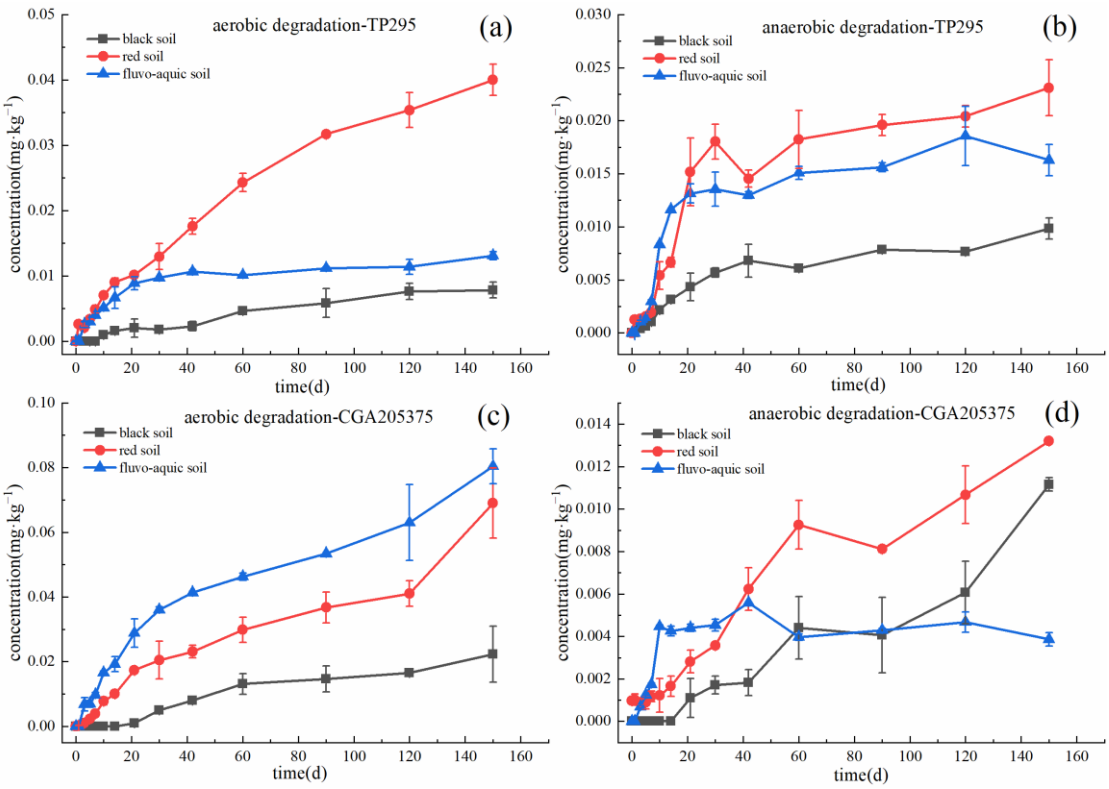

Fig. 3. Dynamic of two degradation products generated from difenoconazole degradation in soil，(a) TP295 under aerobic condition, (b) TP295 under anaerobic condition, (c) CGA205375 under aerobic condition and (d) CGA205375 under anaerobic condition. These compounds were quantified by UHPLC-MS/MS.

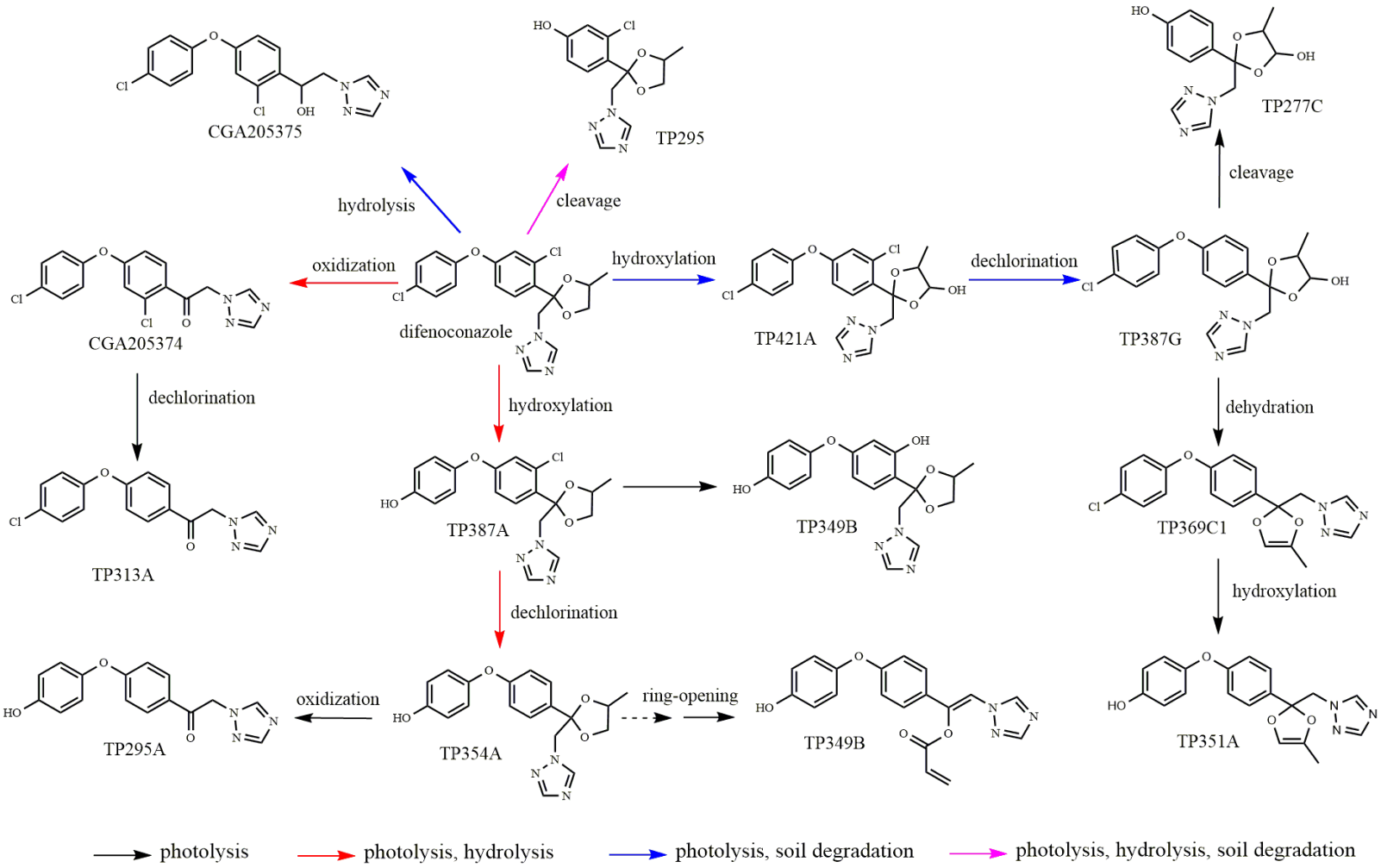

Fig. 4. Proposed pathway for the degradation of difenoconazole in environment.

Supplementary materials

Degradation of difenoconazole in water and soil: kinetics, degradation pathways, degradation product identification and ecotoxicity assessment

Yanli Man [1], Marianne Stenrød [2], Chi Wu [1], Marit Almvik [2], Roger Holten [2], Jihong Liu Clarke [2], Shankui Yuan[3], Xiaohu Wu [1], Jun Xu [1], Fengshou Dong [1], Yongquan Zheng [1,] *, Xingang Liu [1,] *

[1] *State Key Laboratory for Biology of Plant Disease and Insect Pests, Institute of Plant Protection, Chinese Academy of Agricultural Sciences, Beijing 100193, China.*

[2] *Norwegian Institute of Bioeconomy Research (NIBIO), Division Biotechnology and Plant Health, Høgskoleveien 7, 1433 Aas, Norway*

[3] *Environment Division, Institute for the Control of Agrochemicals, Ministry of Agriculture and Rural Affairs, Beijing 100125, China*

* Corresponding author: Prof, Xingang Liu and Prof. Yongquan Zheng, No. 2 West Yuanmingyuan Road, Institute of Plant Protection, Chinese Academy of Agricultural Sciences, Haidian District, Beijing, PR China.

Tel.: +86 10 62815938; fax: +86 10 62815938.

E-mail address: liuxingang@caas.cn (X. Liu), yqzheng@ippcaas.cn (Y. Zheng)

1. preparation of buffer solutions

The pH 4 buffer consisted of 50 mL 0.1 mol·L^{-1} $C_8H_5KO_4$ solution and 0.40 mL 0.1 mol·L^{-1} NaOH solution, which were diluted with pure water to 100 mL. The pH 7 buffer was composed of 50 mL 0.1 mol·L^{-1} KH_2PO_4 solution and 29.63 mL 0.1 mol·L^{-1} NaOH solution, then they were diluted to 100 mL with pure water. 50 mL mixed solution of 0.1 mol·L^{-1} H_3BO_3 and 0.1 mol·L^{-1} KCl and 21.30 mL of 0.1 mol·L^{-1} NaOH solution were diluted to 100 mL with pure water to obtain pH 9 buffer. The pH value was corrected with 0.1 mol·L^{-1} HCl or 0.1 mol·L^{-1} NaOH solution after sterilization. The buffer solutions were freshly prepared prior to use.

2. Degradation kinetic models

Single first order (SFO):$C = C_0 e^{-kt}$. C_t (mg·kg^{-1}) is the concentration at time t and C_0 (mg·kg^{-1}) is the initial concentration, k is the first-order rate constant (h^{-1} or day^{-1}). Consequently, the half-life ($t_{1/2}$) was calculated as $t_{1/2} = \ln 2/k$.

Double first-order in parallel (DFOP): $C = C_0\,(\mathrm{g}e^{-k_1 t} + (1-\mathrm{g})\,e^{-k_2 t})$, g is the distributed fraction of the tested substance that degrades at fast rate (the solution phase). The rate constants k_1 and k_2 corresponds to the fast sub-process (solution phase) and the slow sub-process (sorbed phase) respectively(Briones and Sarmah, 2019).

First order multiple compartments (FOMC): $C_t = \frac{C_0}{(\frac{t}{\beta}+1)^{\alpha}}$, β is a location parameter and α is a shape parameter determined by the coefficient of variation of k values (Bento et al., 2016). The Computer Aided Kinetic Evaluation (CAKE) R-based software was used to obtain the half-lives and degradation rates.

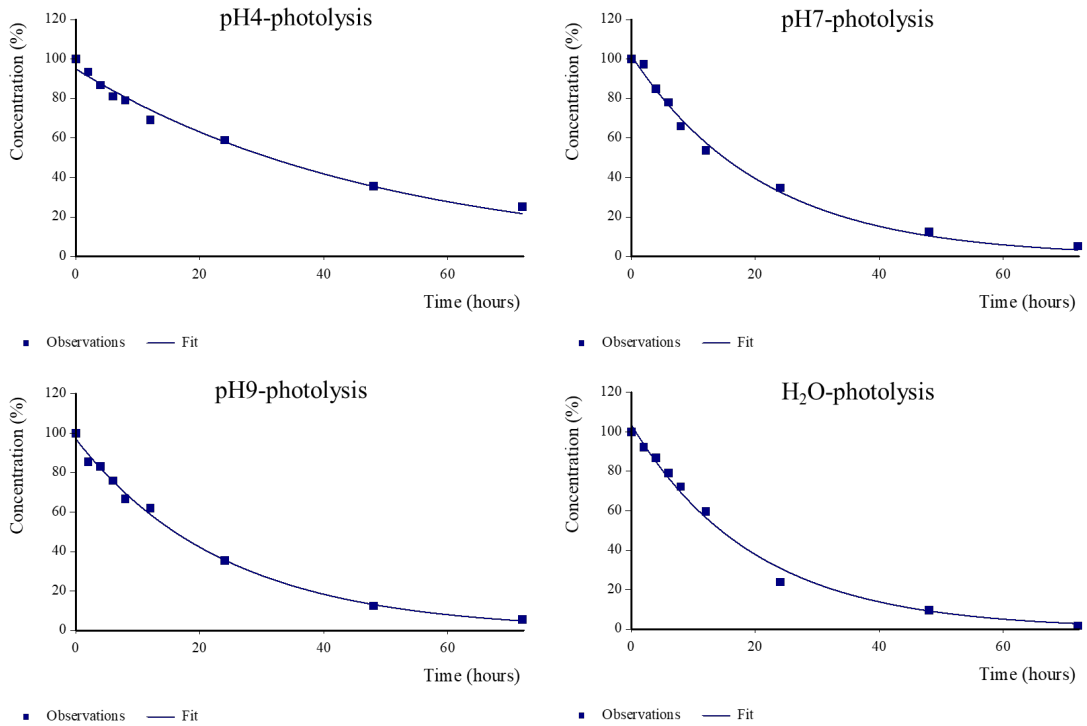

Fig. S1. photolysis kinetics curves (SFO) of difenoconazole in aqueous solutions with different pH values

Table S1. Model outputs from the CAKE model fits to the photolysis data using Single First Order (SFO)

Parameter	pH4 buffer	pH7 buffer	pH9 buffer	H_2O
k (h^{-1})	0.02052	0.04744	0.04173	0.05049
DT_{50} (h)	33.8	14.6	16.6	13.7
DT_{90} (h)	112	48.5	55.2	45.6
R^2	0.9853	0.9934	0.9951	0.9916
χ^2 error (%)	3.4	3.75	3.01	4.46

Table S2. Model outputs from the CAKE model fits to the hydrolysis data using Single First Order (SFO), Double First Order in Parallel (DFOP) and First Order Multiple Compartments (FOMC) kinetic models.

Parameter	pH4 buffer	pH7 buffer	pH9 buffer	H_2O
SFO				
k	0.01665	0.02561	0.01909	0.03249
DT_{50} (d)	41.6	27	36.3	21.3
DT_{90}(d)	138	89.8	121	70.9
R^2	0.9481	0.7915	0.9641	0.8548
χ^2 error (%)	8	20.9	7.38	19.3
SSR	498.8	1625	418.5	1548
DFOP				
k1	0.04272	0.6476	0.03831	0.2103
k2	0.00426	0.01302	0.0016	0.0084
g	0.6087	0.4729	0.7435	0.5915
DT_{50} (d)	31.6	5.79	28	7.7
DT_{90}(d)	320	128	588	168
R^2	0.9836	0.9713	0.9961	0.9982
χ^2 error (%)	4.7	8.06	2.47	2.08
SSR	146	205.3	39.77	15.16
FOMC				
α(SD)	0.9509	0.3379	1.026	0.4632
β(SD)	30.65	0.9893	29.62	2.464
DT_{50} (d)	32.9	6.71	28.6	8.54
DT_{90}(d)	315	900	250	353
R^2	0.9809	0.9679	0.9934	0.9952
χ^2 error (%)	4.82	8.12	3.08	3.28
SSR	170.3	227.6	67.26	41.08

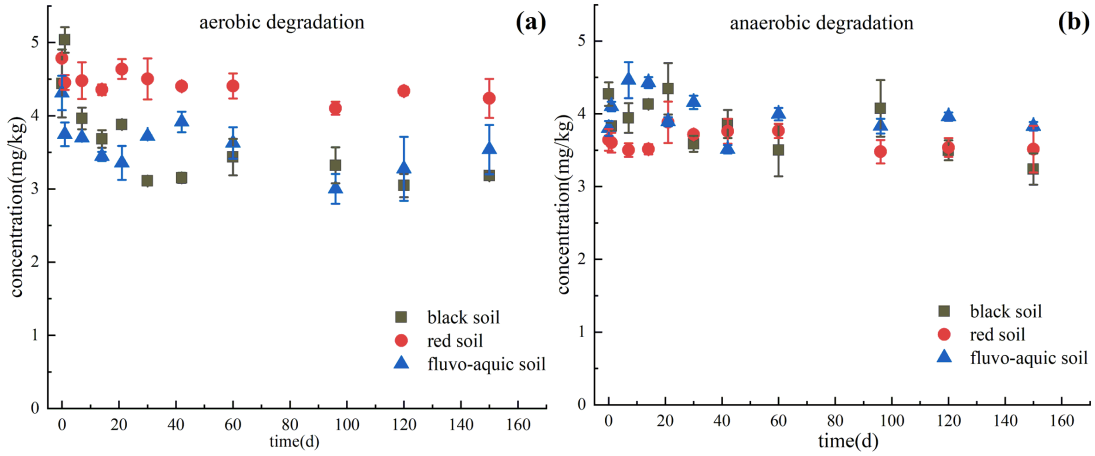

Fig. S2. degradation of difenoconazole in different soils under aerobic (a) and anaerobic (b) conditions.

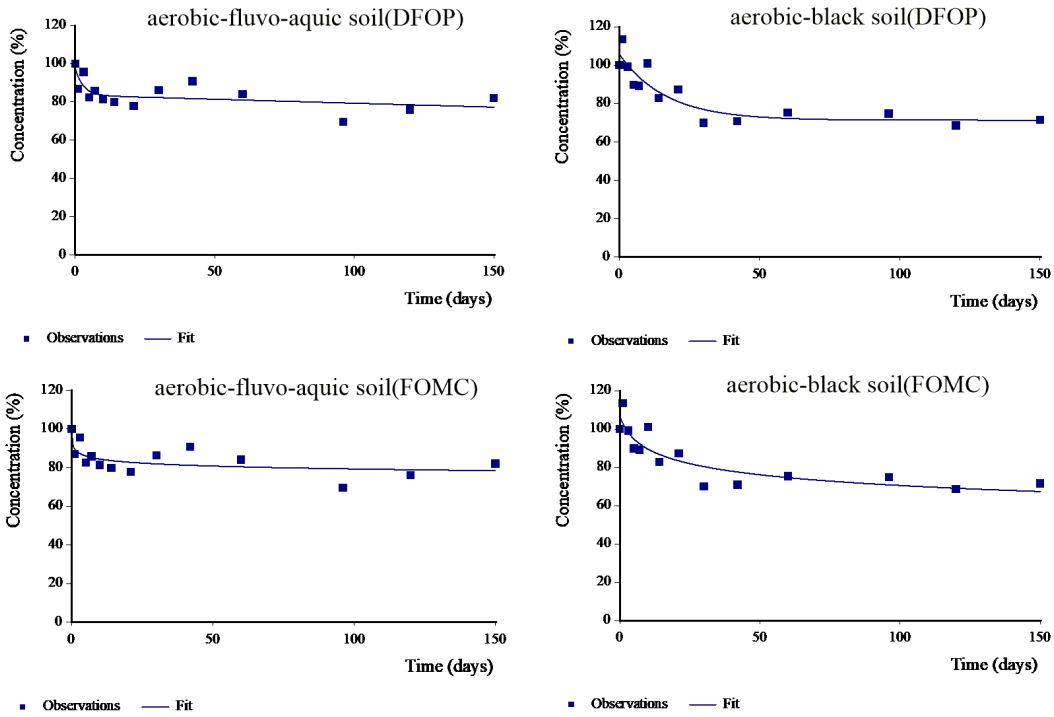

Fig. S3. Double First Order in Parallel (DFOP) and First Order Multiple Compartments (FOMC) kinetic model fits to the data of aerobic degradation in fluvo-aquic soil and black soil.

Table S3. Model outputs from the CAKE model fits to the aerobic soil degradation data using Double First Order in Parallel (DFOP) and First Order Multiple Compartments (FOMC) kinetic models.

Parameter	Fluvo-aquic soil (aerobic)	Black soil (aerobic)
DFOP		
k_1	0.3464	0.06012
k_2	0.00051	0.0031
g	0.1428	0.3245
DT_{50} (d)	-	-
DT_{90}(d)	-	-
R^2	0.5125	0.8267
χ^2 error (%)	5.45	5.82
SSR	386.1	451.3
FOMC		
α	0.0271	0.1145
β	0.01913	2.757
DT_{50} (d)	-	-
DT_{90}(d)	-	-
R^2	0.5183	0.7943
χ^2 error (%)	5.23	6.12
SSR	381.5	536

Table S4. Recoveries (n = 5, %), and RSD (%) for target compounds from different buffer solutions at different spiked levels.

matrix	spiked level ($mg \cdot kg^{-1}$)	difenoconazole			CGA205374			TP295			TP295A			TP354A			TP387A		
		recovery	RSD	LOQ	recovery	RSD	LOQ	recovery	RSD	LOQ	recovery	RSD	LOQ	recovery	RSD	LOQ	recovery	RSD	LOQ
pH4 buffer	0.001	-	-		97.2	13.2		101.6	2.7		97.5	1.7		107.0	4.4		110.8	7.7	
	0.01	98.8	5.8		102.5	6.5		109.7	3.3		107.5	7.4		97.7	8.6		109.3	5.2	
	0.1	98.3	5.1	0.01	98.3	4.4	0.001	112.5	10.2	0.001	114.7	2.5	0.001	97.9.	3.2	0.001	112.5	6.4	0.001
	1	107.4	4.8		105.2	2.3		111.4	5.7		107.4	3.4		100.5	12.7		116.1	1.4	
	5	104.8	3.8		-	-		-	-		-	-		-	-		-	-	
pH7 buffer	0.001	-	-		96.6	9.1		106.5	3.2		102.6	3.2		101.9	16.2		112.6	1.9	
	0.01	96.7	2.9		101.2	6.0		111.4	6.7		118.0	9.5		95.5	8.1		110.3	3.5	
	0.1	99.9	1.5	0.01	99.9	7.3	0.001	114.1	1.6	0.001	105.7	3.2	0.001	98.3	2.6	0.001	99.8	8.1	0.001
	1	105.7	2.7		102.1	2.1		115.9	1.9		111.3	10.5		111.2	7.9		109.0	2.9	
	5	104.1	3.4		-	-		-	-		-	-		-	-		-	-	
pH9 buffer	0.001	-	-		95.3	11.3		96.8	2.6		95.8	1.5		105.0	1.5		101.6	2.4	
	0.01	95.6	6.3		100.9	3.6		110.7	6.8		99.9	2.1		112.2	7.2		108.7	11.6	
	0.1	99.1	3.5	0.01	108.7	7.4	0.001	100.5	2.8	0.001	115.1	5.9	0.001	108.4	5.5	0.001	113.3	3.8	0.001
	1	109.6	2.8		106.7	5.0		99.6	3.7		109.8	3.2		112.1	5.2		118.6	2.8	
	5	102.4	4.7		-	-		-	-		-	-		-	-		-	-	
water	0.001	-	-		99.8	7.5		98.1	5.4		113.8	4.2		101.3	3.8		96.7	11.1	
	0.01	101.3	3.9		108.3	4.2		96.7	1.9		111.3	5.7		104.6	2.7		116.0.	7.0	
	0.1	100.6	3.6	0.01	103.9	4.0	0.001	104.9	5.7	0.001	116.2	1.6	0.001	107.0	9.0	0.001	117.2	5.6	0.001
	1	98.3	4.7		106.6	5.9		113.6	2.7		113.5	2.0		118.6	13.3		109.4	5.3	
	5	104.0	1.8		-	-		-	-		-	-		-	-		-	-	

Table S5. Recoveries (n = 5, %), and RSD (%) for target compounds from different soils at different spiked levels.

matrix	spiked level ($mg \cdot kg^{-1}$)	difenoconazole			CGA205375			TP295		
		recovery	RSD	LOQ	recovery	RSD	LOQ	recovery	RSD	LOQ
Black soil	0.001	-	-	0.01	77.3	2.4	0.001	84.6	4.8	0.001
	0.01	76.0	7.3		80.6	3.3		90.2	1.8	
	0.1	100.1	1.6		82.1	8.0		89.3	3.6	
	1	98.5	4.5		79.2	3.4		97.3	4.4	
	5	92.4	5.0		-	-		-	-	
Red soil	0.001			0.01	82.4	2.9	0.001	88.5	3.6	0.001
	0.01	86.5	9.7		88.3	4.0		99.2	2.2	
	0.1	101.7	4.4		79.1	1.5		102.9	8.4	
	1	109.6	3.4		95.2	6.6		101.8	3.4	
	5	93.0	1.5		-	-		-	-	
Fluvo-aquic soils	0.001	-	-	0.01	75.6	9.1	0.001	96.7	5.5	0.001
	0.01	84.4	10.1		81.1	6.3		80.8	4.1	
	0.1	89.2	7.8		92.3	3.1		105.2	1.7	
	1	92.6	2.4		89.8	2.6		106.2	2.3	
	5	95.1	1.7		-	-		-	-	

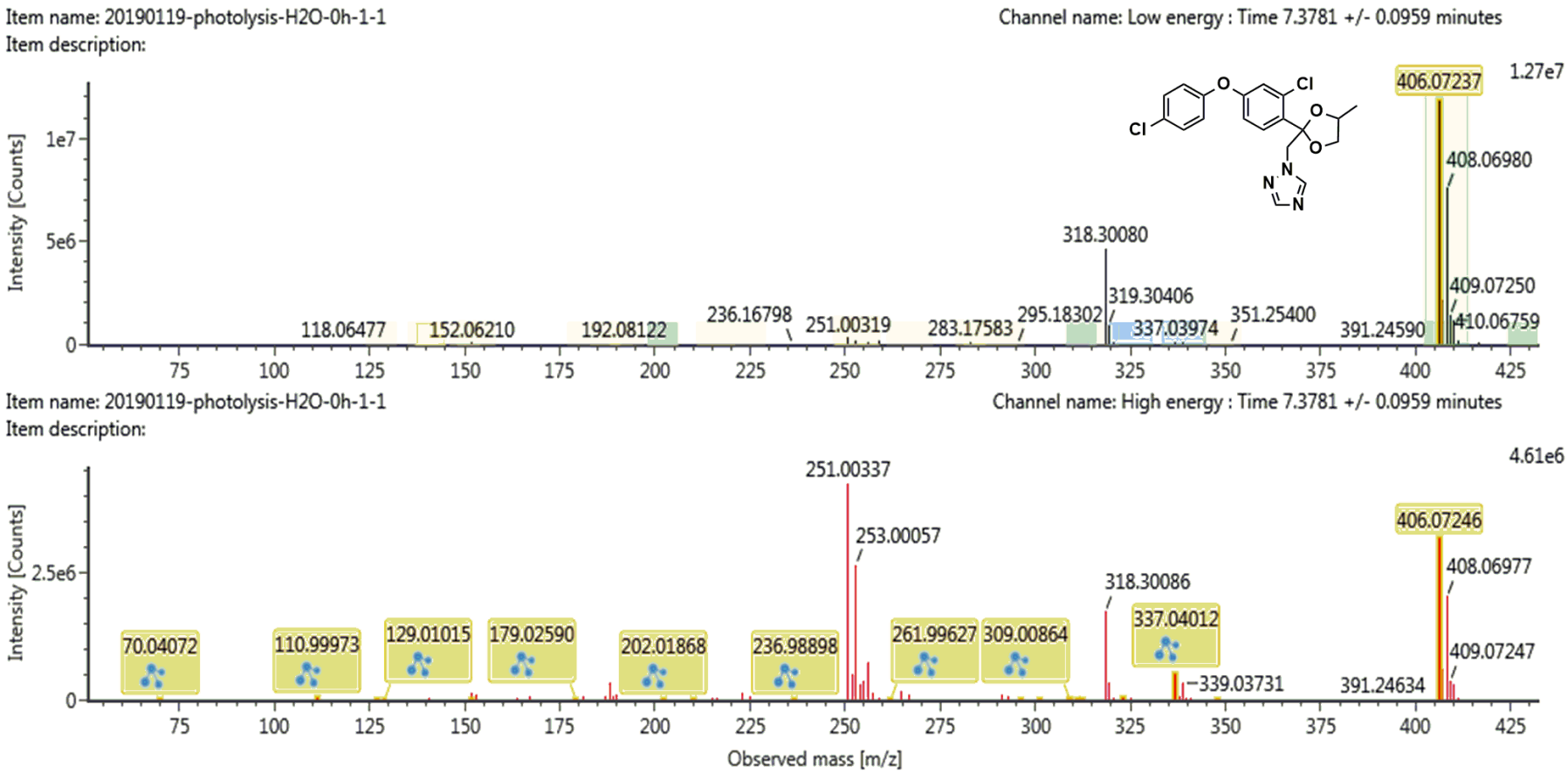

Fig. S4. The spectra and fragmentation pattern of difenoconazole from UNIFI.

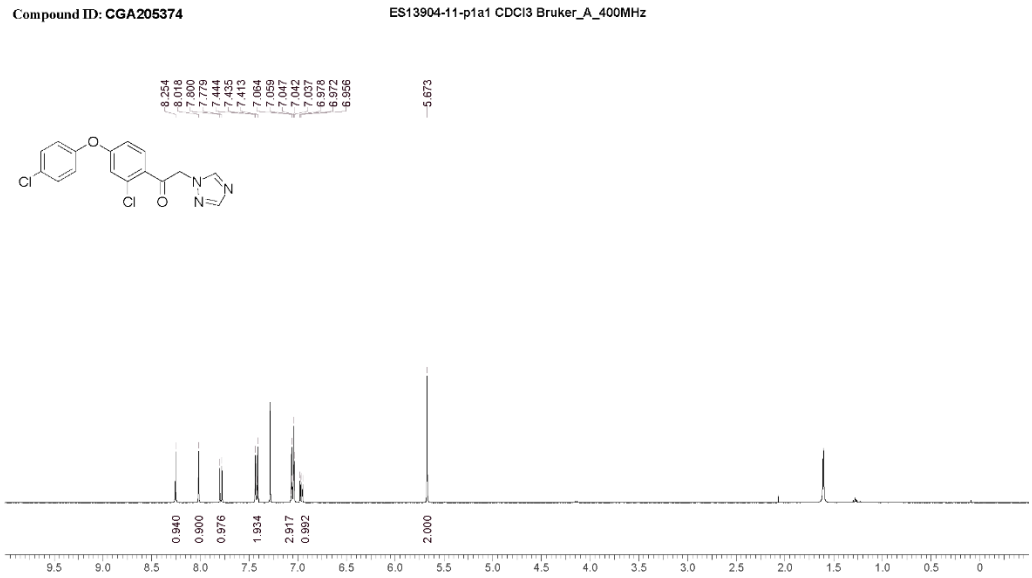

Fig. S5. The ^{1}H-NMR spectrum of compound CGA205374.

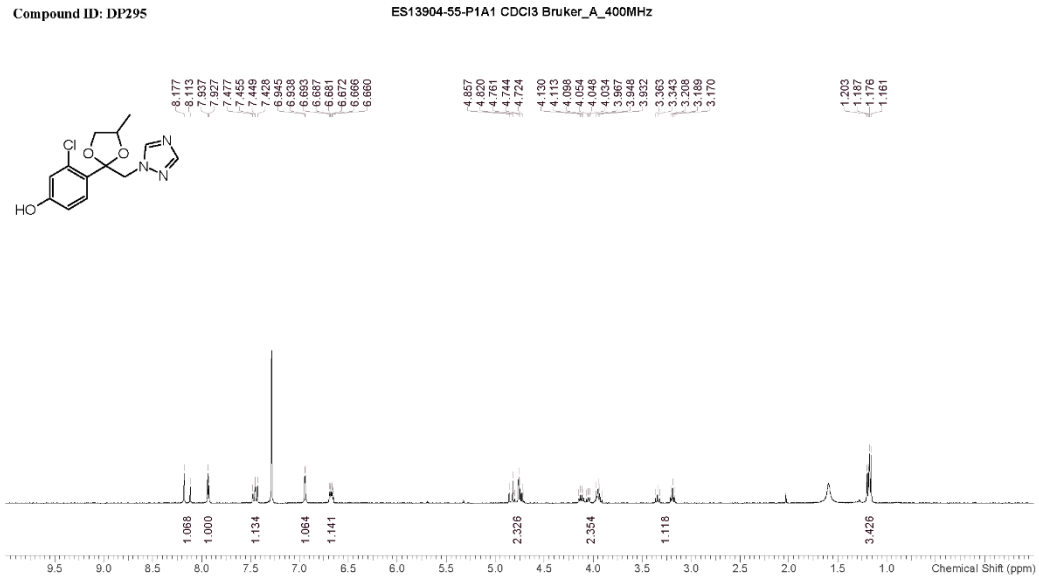

Fig. S6. The ^{1}H-NMR spectrum of compound TP295.

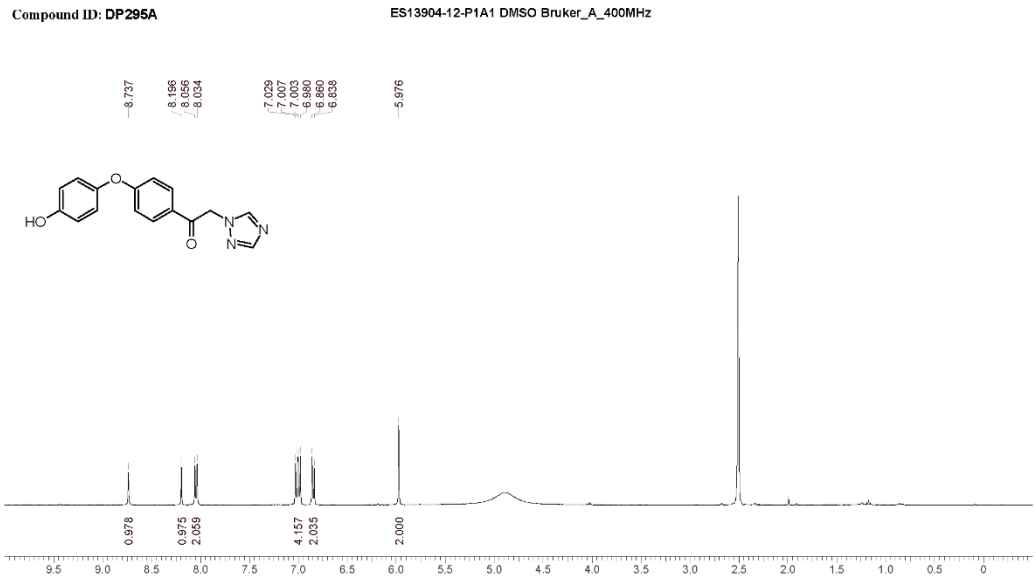

Fig. S7. The ^{1}H-NMR spectrum of compound TP295A.

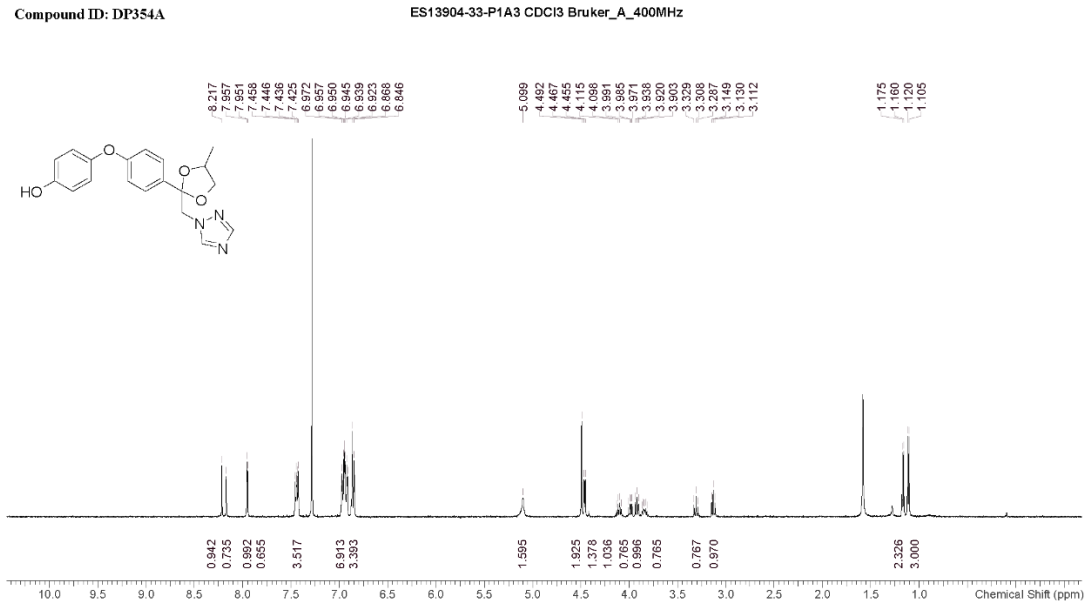

Fig. S8. The ^{1}H-NMR spectrum of compound TP354A.

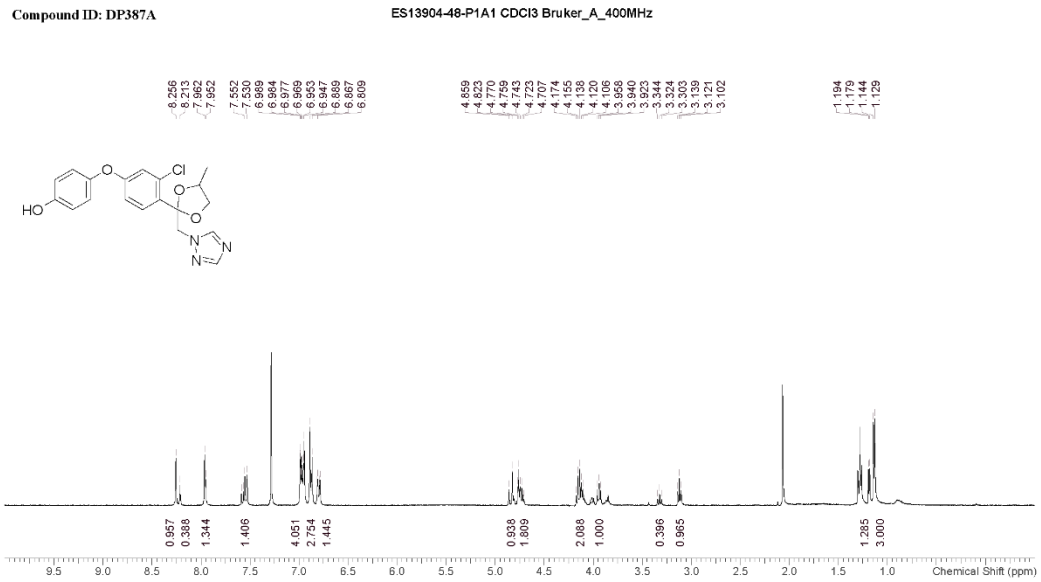

93

94 **Fig. S9.** The ^{1}H-NMR spectrum of compound TP387A.

95

96

Reference

Bento, C.P.M., Yang, X., Gort, G., Xue, S., van Dam, R., Zomer, P., Mol, H.G.J., Ritsema, C.J. and Geissen, V. 2016. Persistence of glyphosate and aminomethylphosphonic acid in loess soil under different combinations of temperature, soil moisture and light/darkness. Science of the Total Environment 572, 301-311.

Briones, R.M. and Sarmah, A.K. 2019. Modelling degradation kinetics of metformin and guanylurea in soil microcosms to derive degradation end-points. Environmental Pollution 245, 735-745.